PERGAMON

Deep-Sea Research II 45 (1998) 1803–1837

DEEP-SEA RESEARCH
PART II

Spatial and temporal dynamics in marine aggregate abundance, sinking rate and flux: Monterey Bay, central California

Cynthia H. Pilskaln[a,*], Charlotte Lehmann[a], Jennifer B. Paduan[b], Mary W. Silver[c]

[a] *University of Maine, School of Marine Sciences, Orono, ME 04469, USA*
[b] *Monterey Bay Aquarium Research Institute Moss Landing, CA 95039, USA*
[c] *University of California at Santa Cruz, Institute of Marine Sciences, Santa Cruz, CA 95064, USA*

Received 2 May 1997; received in revised form 12 March 1998; accepted 13 March 1998

Abstract

Seasonal profiles of marine aggregate abundance and in situ sinking rate experiments were carried out using a uniquely instrumented ROV platform in the midwater column of Monterey Bay California between 1991 and 1994. Variations of an order of magnitude in the midwater 100–500 m abundance of aggregates within the 0.5 to > 5 mm size range were observed on an inter- and intra-annual basis at the study site. Maximum midwater aggregate abundances of 15–40 aggregates l^{-1} were common during the 1991 spring/summer upwelling season, with values of less than 5 aggregates l^{-1} being more typical of the non-upwelling winter months and the 1992 El Niño period. Midwater aggregate peaks represented the temporal signal of sinking aggregate material produced in the overlying waters, with no correlation observed between the vertical distribution of aggregates and the density structure, or the relative suspended particle abundence measured as c_p. Additionally, significant injection of aggregate material to the midwater profiles via lateral advection was not evidenced by the combined aggregate, hydrographic, and physical flow data sets obtained simultaneously at the study site. In situ aggregate sinking rates were measured using an ROV-mounted settling chamber. Mean rates ranged from 16.3 to 25.5 m day^{-1} with a trend of increasing sinking rate with aggregate diameter observed. An analysis of aggregate shape showed a decrease in spherical shape with increasing aggregate diameter and sinking rate. Seasonal aggregate POC fluxes at 450 m for 1991–1992 were calculated from the in situ aggregate property data sets to compare with coincident, 450 m trap-measured POC fluxes. The calculated aggregate POC fluxes ranged from 26.3 to 481.2 $mgC\,m^{-2}\,d^{-1}$ and were at least 1.5–2 times greater than the trap POC fluxes, with the exception of the non-upwelling winter months where values are similar. Trapping efficiency and

* Corresponding author. Fax: 001 207 581 4388; e-mail: pilskaln@maine.maine.edu.

0967-0645/98/$ – see front matter
PII: S0967-0645(98)00053-8

interannual variations in aggregate sinking rates are believed to explain the differences between the aggregate and trap-based POC fluxes.

1. Introduction

In terms of particle mass export in the ocean, the vast majority of sinking particle matter in the ocean exists in the form of particle aggregates, frequently referred to as 'marine snow' or marine aggregates (McCave, 1975; Alldredge and Silver, 1988). The significance of marine aggregates to chemical and biological processes in the world's oceans is strongly a function of aggregate vertical distribution, abundance and sinking rate (Asper, 1987; Alldredge and Gotschalk, 1988, 1989; Gardner and Walsh, 1990; Asper et al., 1992; Walsh and Gardner, 1992; Lampitt et al., 1993; MacIntyre et al., 1995; Davis and Pilskaln, 1993). Aggregate abundance and vertical distribution are substantially influenced by episodic POC production in overlying surface waters on diurnal to seasonal scales, resuspension and horizontal advection, stratification, and turbulent mixing (Alldredge and Silver, 1988; Asper et al., 1992; MacIntyre et al., 1995). Individual aggregate size has been shown to be a particularly important property required for the determination of aggregate settling speed using Stokes' equation (Asper, 1987; Alldredge and Gotschalk, 1989; Walsh and Gardner, 1992). Some investigators have resorted to measuring aggregate settling speeds directly (in situ) due to concerns regarding the ability to accurately estimate aggregate density. This parameter may become of particular importance when attempting to calculate sinking rates of large and highly porous aggregates using Stokes' equation and measured aggregate diameters (Shanks and Trent, 1980; Asper, 1987; Alldredge and Gotschalk, 1989; Syvitski et al., 1995). Results from the above studies employing in situ photographic and SCUBA techniques to measure aggregate properties indicate that substantial temporal and spatial variations may exist in the abundance and sinking rates of marine aggregates, and thus in their mass fluxes through the water column.

Time-series sediment trap studies conducted over the past fifteen years which have been coupled to in situ marine aggregate studies on relatively rare occasions, point to a substantial role for large, fast-settling marine aggregates in the transport of organic nutrients from the surface to the deep ocean (Fowler and Knauer, 1986; Deuser and Ross, 1980; Honjo, 1980; Honjo et al., 1982a; Gardner and Walsh, 1990; Asper et al., 1992; Walsh and Gardner, 1992; Dymond and Collier, 1988). To quantify this transport accurately in a particular marine system, it becomes important to examine specific aggregate properties of abundance, sinking rate, and flux that are coincident in time and space with particulate mass flux measurements. As pointed out in Walsh and Gardner (1992), the numerous assumptions necessary to calculate aggregate mass flux from profiles of aggregate size and abundance may make the correlation between trap fluxes and aggregate profiles possibly fortuitous. These investigators therefore suggested that the appropriateness of such assumptions and calculations may only be determined adequately "when there are sufficient simultaneous data on the temporal variability of (aggregate) profiles, trap fluxes and in situ measurements of aggregate settling velocites" (Walsh and Gardner, 1992).

The study presented here focused on the 100–500 m mesopelagic zone where very few data exist on the variability of marine aggregate abundance and flux as compared to the upper ocean. Additionally, the 100–500 m mid-depth zone, often referred to as the "POC regeneration zone", is where measured POC fluxes are commonly observed to decrease exponentially (Knauer et al., 1979; Martin et al., 1987). Therefore, quantifying the various biogeochemical processes occurring in the 100–500 m regeneration zone is of significant interest to our understanding of marine POC cycling dynamics. Our major objectives in the Monterey Bay study were to determine the seasonal and depth-related variability in midwater aggregate abundance, provide in situ measurements of aggregate sinking rates, and quantify the contribution of marine aggregate POC to the time-varying flux of organic matter below the euphotic zone as measured with a sediment trap. The site chosen for the study, Monterey Bay off central California, presented a high productivity, seasonal coastal upwelling system where we expected to observe strong inter- and intra-annual variations in aggregate abundance and flux (Bolin and Abbott, 1963; Rosenfeld et al., 1994a; Chavez, 1996; Pilskaln et al., 1996). Previous investigators working in the region have observed a high abundance of marine aggregates spanning a wide range of size classes from sub-mm to 10's of cm's in size particularly in the upper water column (Silver et al., 1978; Trent et al., 1978; Shanks and Trent, 1980; Honjo et al., 1984; Davoll and Silver, 1986; MacIntyre et al., 1995). The Monterey Bay region also offered access to a deep water ($>$ 1000 m) study site within several hours from shore thus making it possible to complete monthly to bimonthly aggregate surveys.

2. Methods

2.1. Study site

All marine aggregate measurements and collections were completed at a 1600 m-deep site located at the outer edge of Monterey Bay (Fig. 1). The seasonal upwelling dynamics of this western boundary system and the resultant geochemical and biological effects are detailed in Rosenfeld et al. (1994a), Chavez (1996), and Pilskaln et al. (1996). Upwelling occurs primarily between the end of February to October with intermittent periods of enhancements and relaxations in response to local wind forcing and interactions with the California Current (Bolin and Abbott, 1963; Rosenfeld et al., 1994a). Periods of maximum upwelling from approximately March to August are reflected in the cold, salty, nutrient-rich water in the near-surface waters of the Bay, and in the elevated rates of integrated primary production and chlorophyll levels measured within the euphotic zone during this period (Rosenfeld et al., 1994a; Chavez, 1996). A time-series sediment trap mooring deployed from 1989 to 1992 was located approximately 2 km north of the marine aggregate study site. Biweekly particulate flux data sets obtained from a 450 m trap on the mooring, as well as data from mooring-mounted current meters, were made available to the present study (Pillsbury et al., 1992; Pilskaln et al., 1996).

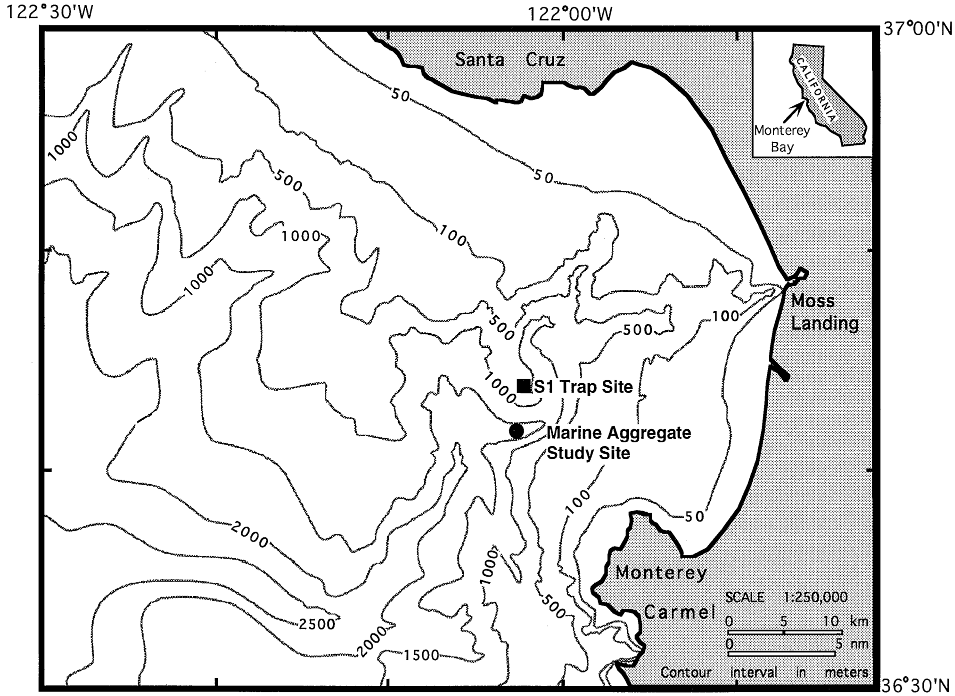

Fig. 1. Study location in Monterey Bay, central California. Marine aggregate site (filled square) and 1989–92 S1 time-series sediment trap mooring site (filled circle; Pilskaln et al., 1996) are shown.

2.2. ROV platform and aggregate size and abundance surveys

Measurements of aggregate properties of size and abundance were completed during 1991 and 1992 using specialized instrumentation mounted to the Monterey Bay Aquarium Research Institute's (MBARI's) remote operated vehicle (ROV) 'Ventana', a Hysub 1850 manufactured by International Submarine Engineering, Ltd. of British Columbia (Pilskaln et al., 1991; Robison, 1993; Davis and Pilskaln, 1993). The marine aggregate measurement system developed for determining the in situ size distribution and abundance of water column aggregates has been described in detail in Pilskaln et al. (1991) and Davis and Pilskaln (1993). The essential units of the system are a high resolution video camera coupled to a paired, structured light unit (Fig. 2). The camera used in this study was a Sony DXC-3000 color video camera with a Fuginon zoom lens; the structured light unit was composed of two zoomable and focusable Sea Projector Lamps from Deep Sea Power and Light, Inc. (Davis and Pilskaln, 1993). A well-defined structured light volume was created by a pair of continuous light beams from the Sea Projector Lamps that were "structured" by rectangular masks within each of the lamp housings units. The two structured light beams were deflected by a pair of exterior mirrors to produce an intense beam that was located 1 m in front of, and at a 90° angle to, the camera's field of view (Fig. 2).

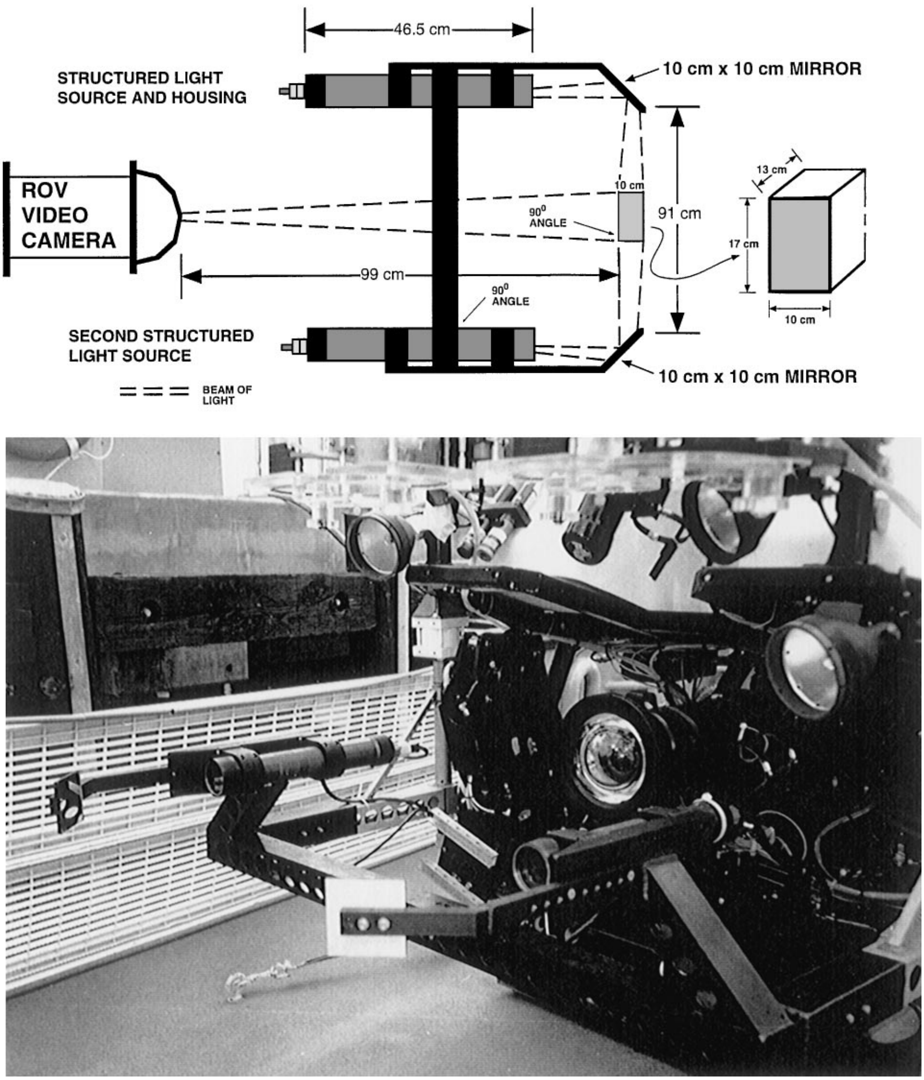

Fig. 2. Schematic of structured light/video system used in the study. Photograph shows system mounted on the MBARI ROV for water column surveys of aggregate abundance. Bottom of the four HBOI detritus samplers used to sample aggregates in the study are seen at the top of the photograph.

The video camera's field of view was represented by a 2.2 l, 17 cm (length) $\times$ 10 cm (width) $\times$ 13 cm (height) portion of the total structured light volume (Fig. 2). The camera's focal distance and depth of field were calibrated in a test tank using commercially available plastic beads of known size. This ensured that any aggregate occurring within the 10 cm thickness of the imaged beam was in focus with a $< 2\%$ change in the apparent aggregate size between the front and back of the structured light volume (Davis and Pilskaln, 1993). Aggregates were illuminated and imaged as they passed through the defined structured light volume on slow moving (3.0 m min^{-1} average speed), horizontal ROV transects. For the study presented here, horizontal ROV transects for aggregate size and abundance data collection were conducted at 25 m intervals between approximately 100 and 500 m on fifteen 1991–92 cruises to the Monterey Bay study site. Each transect was 1 min in length with the total water volume surveyed at each depth equal to 66.3 l.

A SeaBird CTD (model SBE-9) and SeaTech transmissometer (25 cm pathlength, 660 nm light source) were mounted on the ROV for all aggregate transects to provide depth profiles of hydrographic and beam attenuation characteristics. Salinity, density (as potential density anomaly, sigma-theta), and potential temperature were calculated as in Fofonoff and Millard (1983) and according to the MBARI CTD data processing procedures detailed in Rosenfeld et al. (1994b). The transmissometer was routinely (monthly) calibrated in air and particle-free water according to the SeaTech manual procedures, and total beam attenuation was corrected for attenuation due to water and DOM (yellow matter) to yield attenuation due to particles only, termed c_p (Bishop, 1986; Pak et al., 1988; Sea Tech Inc., 1995). Dissolved oxygen was measured with a Sea-Bird oxygen sensor incorporated into the pumped flow system on the parent SBE-9 CTD (mounted on the ROV), with data processing completed using the standard SeaBird software package (D. Bracher, personal communication). Monthly calibration of the O_2 sensor was completed using bubbled N_2 in an enclosed sealed recirculating system and cross-calibration was periodically completed via correlation to water samples analyzed by Winkler titration for dissolved oxygen (Parsons et al., 1984; D. Bracher, pers. comm.). All ROV CTD, transmissometer, and dissolved O_2 data were collected at 1 second intervals, with despiking and preliminary processing of the data sets conducted according to the routine MBARI procedures outlined in Rosenfeld et al. (1994b).

Daytime quantitative surveys and sampling of marine aggregates in the midwater were completed on seven cruises in 1991 and eight cruises in 1992 using the MBARI research vessel Point Lobos. In August 1992, two night cruises were conducted to examine aggregate abundance in relation to upper water column hydrographic structure and suspended particle abundance. Night-time aggregate surveys of the upper water column aggregate properties were necessitated by the fact that ambient sunlight interfered with the structured light field above a depth of 50–75 m during the day. All video imagery on the cruises was collected on time-coded, Beta format videotapes and returned to shore for processing.

Quantitative processing of the videotapes for aggregate size and abundance at each depth surveyed was accomplished using a 12-bit overlay frame grabber board (from Imaging Technology) and the Optimas, Inc. image processing software package (Davis and Pilskaln, 1993). Both were placed on a Windows 3.0 based PC and interfaced to a JVC Beta videotape player with dynamic tracking to allow for frame-by-frame analysis (Davis and Pilskaln, 1993). For each 1 min horizontal transect conducted at the 25 m depth intervals, individual frames (each representing 2.2 l) were grabbed and analyzed every 2 seconds for numbers of aggregates within six size classes. This procedure resulted in 30 data sets of size and abundance for each transect depth.

Aggregate size was defined by its longest dimension which placed the aggregate within one of six size classes designated in the present study as classes A–F of increasing aggregate size: 0.5 to < 1.0, 1.0 to < 2.0, 2.0 to < 3.0, 3.0 to < 4.0, 4.0 to < 5.0, and $\geqslant 5.0$ mm (Davis and Pilskaln, 1993). These aggregate size classes match those previously used to define "marine snow" based on SCUBA and submersible observations (Alldredge and Gotschalk, 1988; Alldredge and Silver, 1988). Individual aggregate volumes also were determined with the Optimas program. This was accomplished by measuring the aggregate dimension perpendicular to the longest dimension and using the two measurements to calculate an ellipsoid volume. Assumption of ellipsoidal aggregate volume was based on many hours of videotape examination in which we noted that a substantial number of aggregates could be best described as ellipsoids, not spheres. Application of the ellipsoid volume formula would obviously not result in any volume calculation errors if in fact an aggregate was spherical in shape.

2.3. In situ aggregate sinking rate determinations

In situ sinking rates of aggregates were measured in a 30 cm $\times$ 30 cm $\times$ 60 cm (54 l) plexiglass sinking chamber mounted to the front of the ROV on five cruises between August 1993 and February 1994 (Fig. 3). The aggregate sinking chamber was mounted in such a manner to allow the structured light beam to shine unimpeded through the center of the chamber volume. ROV video camera zoom and focus settings were maintained at the same settings as for the aggregate size and abundance surveys to provide focused imaging of the same 2.2 l, 17 cm $\times$ 13 cm $\times$ 10 cm volume of water which represented 4% of the total chamber volume (Fig. 3). Sinking experiments were conducted at 100 m intervals between 100 and 500 m on five cruises to the aggregate study site in 1993–94. During the experiments, the hydraulically-operated fore and aft plexiglass chamber doors were deployed in the open (or "up") position. Upon reaching the desired depth, the ROV would sit neutrally buoyant in the water column for a few minutes, then move ahead slightly as the chamber doors enclosed a volume of water and aggregates by sliding down vertically into the closed position (Fig. 3). At this point the vehicle would stop moving and maintain its position at the sample depth. After enclosing the water volume, the motion of aggregates contained within the 2.2 l structured light volume inside the chamber was recorded on videotape over a 20–40 min period.

For each videotaped sinking rate experiment, one video frame every 15 s was analyzed by the PC-based image processing system to quantify the change over time in the aggregate size distribution within the chamber. Sampling the videotape every 15 s, with a view area height of 13 cm (height of the structured light volume), allowed us to potentially view all aggregates sinking at rates of less than 750 m d^{-1}. It was assumed that the time-dependent change within each aggregate size class would represent a decrease in the abundance of aggregates primarily due to sinking versus turbulence in the chamber. Thus the aggregate loss rate could be used to approximate a sinking rate for each aggregate size class at each experiment depth. During the initial design of the chamber we consulted with T. Osborn (Johns Hopkins University) to

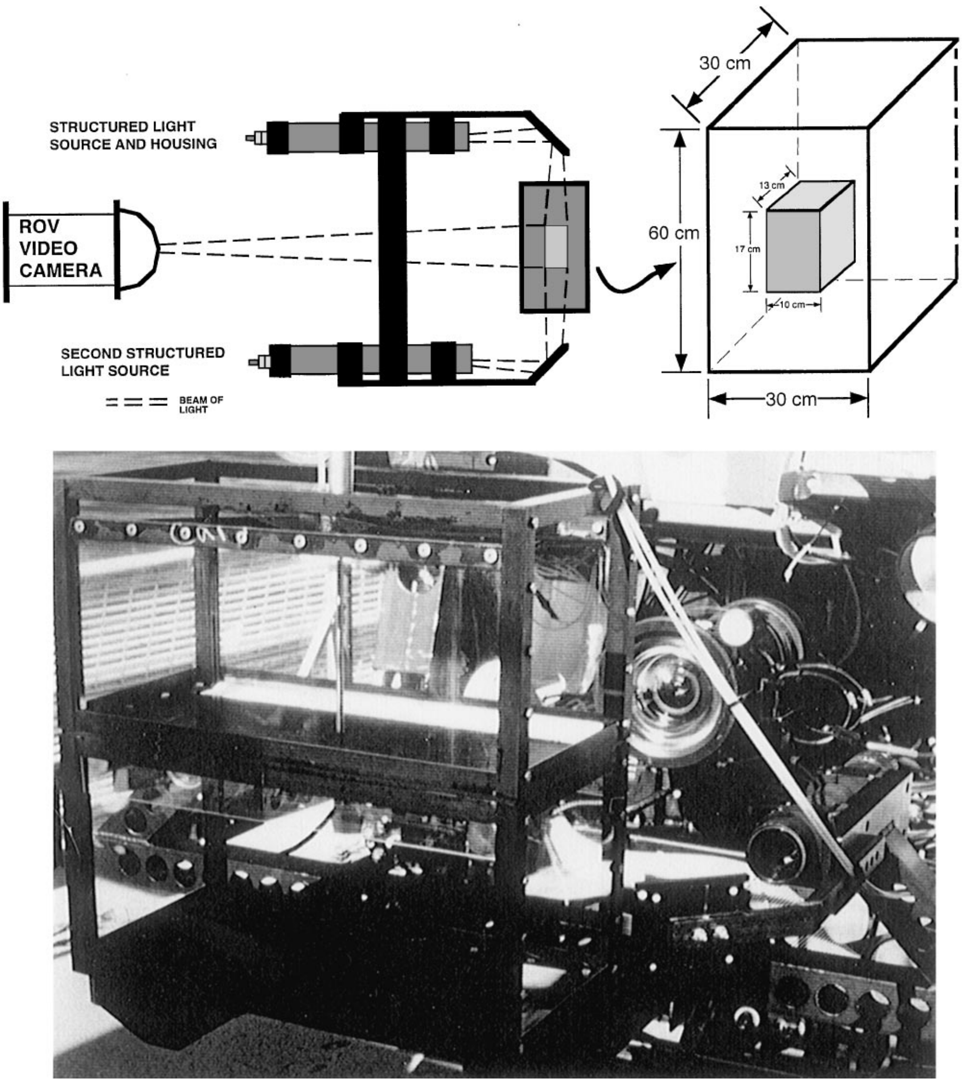

Fig. 3. Schematic of the structured light/video system configured with the plexiglass aggregate sinking chamber used to measure in situ settling rates of midwater aggregates. Physical dimensions of structured light unit and all camera/light angles same as in Fig. 2. Photograph shows sinking chamber mounted to ROV with the large fore and aft chamber doors open. Upper chamber "box" provides structural support for hydraulically operated doors; actual sinking chamber is lower box. Lower edge of the forward plexiglass door of settling chamber is visible near the top of the lower box.

determine the optimal chamber size for minimizing turbulent edge effects that might impinge upon the central portion of the structured light volume (Fig. 3). We observed during the course of the first sinking rate experiments that minor to moderate levels of turbulent motion of the particles contained within the chamber were unavoidable, introducing some error into the trend of decreasing aggregate abundance with time. In order to dampen the effect of such error on the overall aggregate loss rate signal, a least-squares regression was applied to the data sets of aggregate abundance versus time (for each size class) to quantify the underlying loss trend. As a first approximation of aggregate sinking rate, we used the best fit regression line to determine the time required to reduce by half the aggregate abundance in each size class within the viewed volume. This method was arrived at by assuming an even particle distribution throughout the chamber, a column of sinking aggregates that initially extended from the top of the chamber through the structured light volume which we viewed, and a resupply of aggregates from the area of the chamber above the light volume. Calculation of sinking rate in this manner does not require the assumption of a uniform sinking rate for all aggregates within the same size class as we are examining only the decrease in the size class abundance over time as a function of sinking. Therefore, the sinking rate determined for each size class is a true average for the natural population.

In addition to the measurement of size obtained for all aggregates involved in the sinking rate experiments, a measure of aggregate circularity was determined for a subset of these aggregates using the Optimas program. Circularity was simply defined as P^2/A, where P is equal to a measurement of an aggregate's perimeter and A is the area of the aggregate viewed and calculated as a polygon. We made these measurements in the interest of determining how closely aggregates approach the shape of a circle in two dimensions, and thus by inference, a sphere in three dimensions. If an aggregate has a circular shape, then the circularity value is equal to 12.57 or 4 pi. All circularity values greater than this represent aggregate shapes that are increasingly less circular or spherical. Our objective in completing this measurement on the aggregates for which we also had size and sinking rate data, was to identify any trends in aggregate shape change associated with aggregate size, sinking rate, and sinking depth.

2.4. Sampling and chemical analyses of aggregates

Samples of midwater marine aggregates and surrounding water were obtained on five cruises to the study site in 1992 and 1993. Four 7.5 l HBOI (Harbor Branch Oceanographic Institute) acrylic detritus samplers mounted above the structured light/video camera system on the front of the ROV were used to collect aggregates (Fig. 2; Robison, 1993). The samplers had hydraulically operated, top and bottom closing doors that allowed for a volume of water containing aggregates to be easily enclosed within the cylindrical samplers at depth. Rubber gaskets lining the sampler doors prevented leakage of the contained sample. Immediately upon recovery of the ROV, the detritus samplers were removed from the vehicle and placed in a shipboard laboratory where individual aggregates were carefully pipetted out of the samplers and counted from each sampler. Aggregate samples were placed in 4% buffered formalin solution and returned to shore for organic carbon analysis by a UIC, Inc. Full Carbon System Coulometer according to the procedures detailed in Pilskaln and Paduan (1992). Aggregates from each sample depth per cruise were combined and filtered onto combusted, pre-weighed GF/F filters, rinsed with Milli-Q water, dried, weighed, and fumed with 12 N HCl for 24 h prior to the coulometric carbon analysis. Filter blanks were treated in the same manner.

3. Results

3.1. Spatial and temporal trends in marine aggregate abundance and size distribution

Significant inter- and intra-annual variability was observed in the 1991–92 trends of marine aggregate size and abundance in the midwater depths of Monterey Bay (Figs. 4 and 5). Highest aggregate abundance values of up to 48 aggregates l^{-1} and aggregate volumes exceeding 30 $mm^3 l^{-1}$ were observed in the spring and summer months of 1991, coincident with the onset of the upwelling season, and the period of maximum primary productivity and high POC fluxes (Chavez, 1996; Pilskaln et al., 1996). Minimal aggregate abundances of < 5 aggregates l^{-1} were documented in the water column in 1991 during the non-upwelling, winter months of January and December (Fig. 4). The aggregate data sets presented in Figs. 4 and 5 represent the mean values obtained from the analysis of 30 images sampled from the one minute horizontal transects completed at each 25 m depth interval. Horizontal variability in aggregate abundance was equal to the standard deviation of the total number of aggregates per liter determined at each survey depth. This varied from a minimum of approximately 10% for depths where total aggregate abundance was greater than or equal to 15 aggregates l^{-1}, to a maximum of 50% for depths where aggregate abundance was less than 2 aggregates l^{-1}.

Substantially lower abundance values and volumes of marine aggregates were evident within the Monterey Bay water column in 1992 as compared to 1991 (Figs. 4 and 5). The decrease in aggregate abundance in 1992 reflected the impact that the 1992 El Niño year had on the chemical and biological character of the Monterey Bay water column (Chavez, 1996; Pilskaln et al., 1996). Relative to 1990–91, 1992 sea surface temperatures were elevated in the Bay, surface nitrate concentrations were reduced, lower primary productivity rates and algal biomass levels were evident, and a resultant reduction in the production and export of organic phytodetritus was observed (Chavez, 1996; Pilskaln et al., 1996; Figs. 4 and 5).

In terms of aggregate size, the dominant classes were the 0.5 to < 1.0 and 1.0 to < 2 mm aggregate classes, representing over 90% of the total aggregates at any depth in any season over the 1991–92 size and abundance survey period (Fig. 4).

Fig. 4. 1991–1992 time-series profiles of mid-water aggregate abundance (number l^{-1}) within six aggregate size classes measured at the Monterey Bay study site. Center panels between the 1991 and 1992 aggregate profiles display 0–300 m temperature record from Monterey Bay, 1991 and 1992 (Chavez et al., 1994; Chavez, 1996). 1991 record shows evidence of normal spring upwelling in spring/early summer months with 11°C water (blue) located at or near the surface. Upwelling ceased at the end of summer/fall with warm 14–16°C water (yellow-red) forming a surface layer. Comparison of the 0–300 m temperature structure of 1991 versus El Niño year 1992 shows warm waters of $\geqslant 14°$ evident at the surface throughout 1992 (Chavez, 1996). Midwater aggregate abundance values decreased overall from 1991 to 1992.

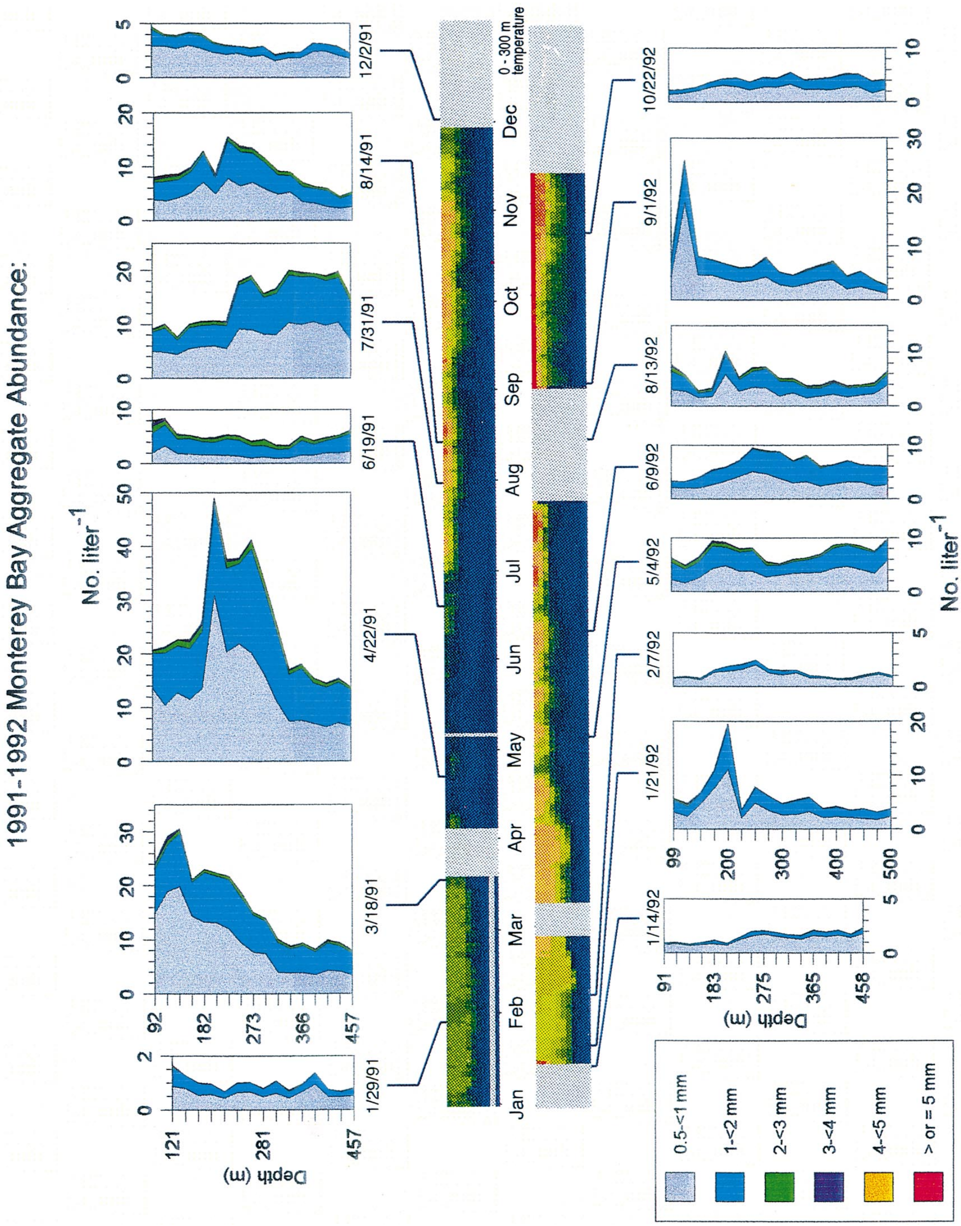
1991-1992 Monterey Bay Aggregate Abundance:
No. liter-1
Depth (m)
1/29/91
3/18/91
4/22/91
6/19/91
7/31/91
8/14/91
12/2/91
1/14/92
1/21/92
2/7/92
5/4/92
6/9/92
8/13/92
9/1/92
10/22/92
Jan
Feb
Mar
Apr
May
Jun
Jul
Aug
Sep
Oct
Nov
Dec
0 - 300 m temperature
0.5-<1 mm
1-<2 mm
2-<3 mm
3-<4 mm
4-<5 mm
> or = 5 mm

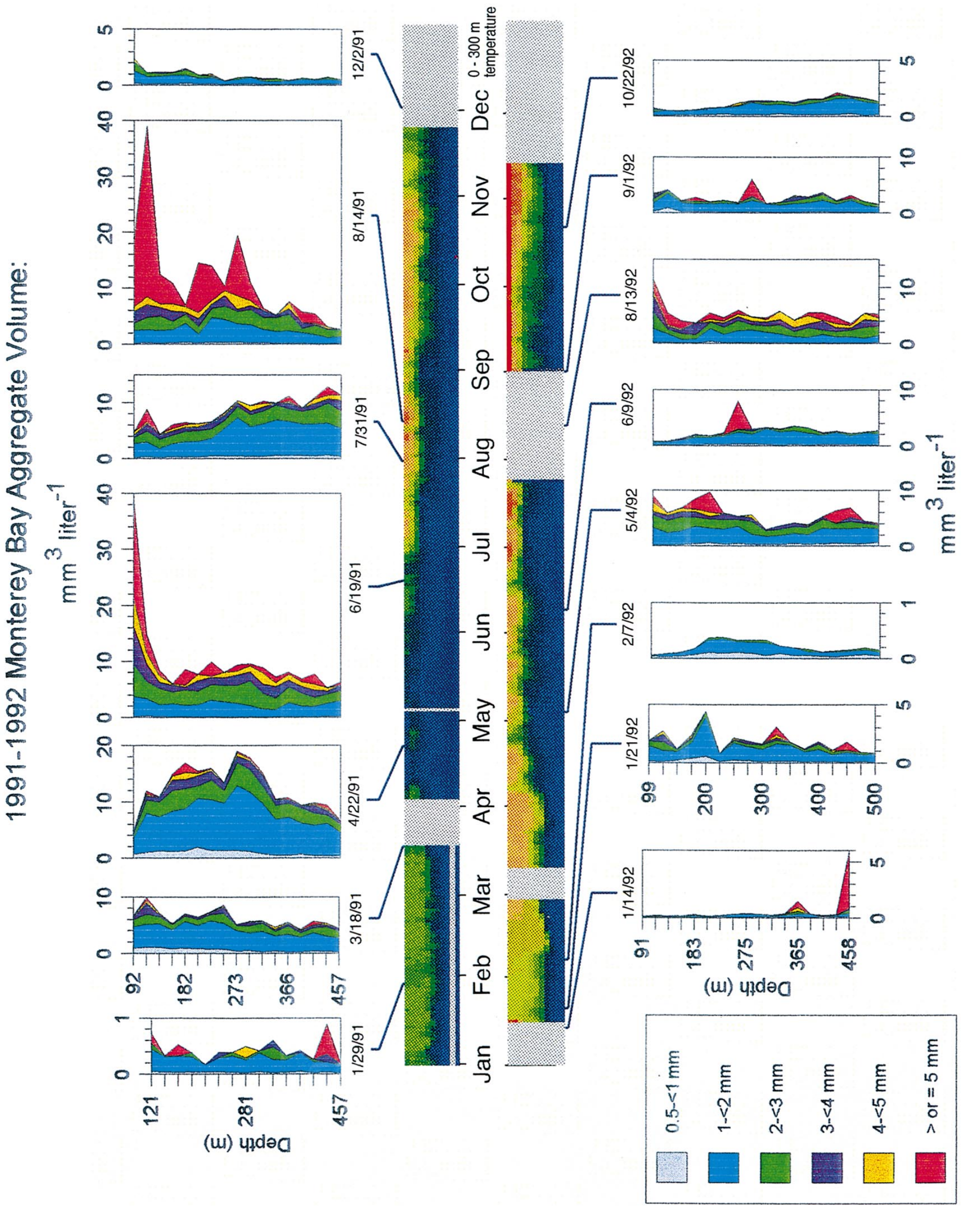
1991-1992 Monterey Bay Aggregate Volume:
mm3 liter-1
0 - 300 m temperature
1/29/91
3/18/91
4/22/91
6/19/91
7/31/91
8/14/91
12/2/91
1/14/92
1/21/92
2/7/92
5/4/92
6/9/92
8/13/92
9/1/92
10/22/92
Jan
Feb
Mar
Apr
May
Jun
Jul
Aug
Sep
Oct
Nov
Dec
Depth (m)
0.5-<1 mm
1-<2 mm
2-<3 mm
3-<4 mm
4-<5 mm
> or = 5 mm

Where midwater numerical aggregate peaks occurred (as number l^{-1}), the contribution by these two size classes was either equally split between the two or the 0.5 to < 1.0 mm class dominated (Fig. 4). We defined a peak in numerical aggregate abundance as a 25% or more increase in the abundance relative to that obtained at the survey depth immediately above where the aggregate abundance began to increase (e.g. after MacIntyre et al., 1995). The occurrence of aggregates from the larger size classes, especially those greater than 3 mm in size, resulted in large peaks in total aggregate volume (Fig. 5). Of particular note was the fact that the presence of $\geqslant$ 5.0 mm-sized aggregates at abundance levels of only 0.20–0.25 aggregate l^{-1}, produced significant aggregate volume peaks as apparent in the 6/19/91 and 8/14/91 profiles between 92 and 113 m (Fig. 5). Overall, the abundance of larger (> 3.0 mm) aggregates was significantly less during the 1992 El Niño year as compared to 1991.

3.2. *Depth trends in aggregate abundance: Relationship to hydrography and lateral resuspension*

Depth-related trends in aggregate size and abundance were most pronounced during the spring/summer months of 1991–92, with the late fall-winter months displaying relatively flat depth profiles (Figs. 4 and 5). When peaks in aggregate number or volume occurred, they were primarily concentrated in the 100–275 m depth interval, with the largest peaks observed between 180 and 275 m in 1991 (Figs. 4 and 5). Coincident CTD and dissolved oxygen data sets were successfully collected for seven out of the 15 midwater aggregate surveys, with transmissometer data available for four of the seven. Representative profiles of the water column properties along with the midwater aggregate abundance profiles (Fig. 6a and b) illustrate the featureless water column density structure in Monterey Bay between 100 and 500 m documented previously by other researchers (i.e. Rosenfeld et al., 1994b). No correlation was observed between the trends of midwater aggregate abundance and beam attenuation due to suspended particles (c_p), or the hydrographic properties of dissolved oxygen, salinity, potential temperature, and density in any of the seven surveys where all of the above properties were measured simultaneously.

Results from two upper water column (0–100 m) aggregate surveys completed in August 1992, however, did show aggregate abundance peaks associated with strong density discontinuities (Fig. 7a and b). In both the August 27 and 28 night-time surveys, the depths of the shallow aggregate peaks correspond to the base of the pycnocline, thermocline, and the c_p minimum (Fig. 7a and b). Based on a 1990–92 marine snow study conducted at a number of sites off central California, MacIntyre et al. (1995) suggested a strong correlation between the occurrence of marine aggregate abundance peaks and the presence of density discontinuity layers in the upper water column. The authors showed that the accumulation of marine aggregates at

◄———

Fig. 5. 1991–1992 time series of mid-water aggregate volume ($mm^3\ l^{-1}$) within the six size classes examined at the aggregate study site. Size class color designations and central temperature panels are the same as in Fig. 4. Aggregate volumes were significantly less during the 1992 El Niño as compared to 1991, especially during the spring and summer months.

density discontinuities in the upper 100 m was the combined result of increased turbulent mixing at the top of such layers resulting in an accumulation of small aggregates, and a significant decrease in aggregate sinking speed for larger, highly porous aggregates as they sank into denser waters (MacIntyre et al., 1995). Even though our upper water column aggregate abundance data set was limited to only two profiles, it would appear reasonable that the above mechanisms offer plausible explanations for the occurrence of aggregate abundance peaks coincident with obvious density features observed in the upper 100 m of Monterey Bay.

The lack of any clear correlation between the spring/summer midwater (100–500 m) aggregate peaks and the coincident hydrography leaves us with two possible explanations for the primary origin of these aggregate peaks: either they resulted from horizontal advection or they represent the temporal signal of a sinking aggregate population recently produced in the overlying water column (e.g. Asper et al., 1992). Midwater lateral advective input of aggregates at our study site from adjacent slope areas is at first glance a reasonable suggestion due to the fact that the study was conducted in an offshore coastal region, located over the Monterey Canyon (Fig. 1). Several lines of evidence however indicate that such input was minimal in regards to its effect on the total abundance of marine aggregates examined in the present study.

Continuous flow data obtained from current meters deployed between 418 and 506 m from August 1989 to November 1991 at the S1 sediment trap site (2 km north of the aggregate study site, Fig. 1) revealed mean, low-pass filtered flows that did not exceed 3 m s^{-1} (Pillsbury et al., 1992). Additionally, results from several other studies of the physical flow field in the upper and midwater column of Monterey Bay characterize the region as one in which mean surface/near surface currents are strong (frequently 10 to 20 cm s^{-1} or greater) and predominantly southward and offshore. Flows greatly diminish below approximately 100 m, and lateral flow velocities across the edge of Monterey Canyon are reported to be primarily tidal on the order of 5–9 cm s^{-1} (Broenkow and McKain, 1972; Rosenfeld et al., 1994; Paduan and Rosenfeld, 1996). The absence of energetic and persistent mid-depth flows, coupled with the lack of depth-related trends in the midwater c_p and aggregate abundance profiles, suggest that midwater advection of particulate sedimentary material from adjacent slopes did not exert a major influence on the structure of the aggregate abundance profiles.

The S1 time-series sediment trap samples collected in Monterey Bay from 1989 to 92 provided some additional support for the primarily near-surface/planktonic origin of the midwater aggregate peaks versus a resuspension/advection source. Pilskaln et al. (1996) reported that the spring/summer S1 trap material collected adjacent to the aggregate study was dominated in 1990 and early 1991 by phytodetritus and diatom-packed fecal pellets in which the phytoplankton exhibited minimal signs of degradation. During the spring/summer of the 1992 El Niño year, the relatively

Fig. 6. Examples of daytime aggregate abundance profiles with hydrographic/particle beam attenuation (c_p) data sets, 7/31/91 and 1/21/92. No correlations were observed in Monterey Bay between features in the aggregate abundance profiles and coincident 100–500 m hydrographic or c_p profiles.

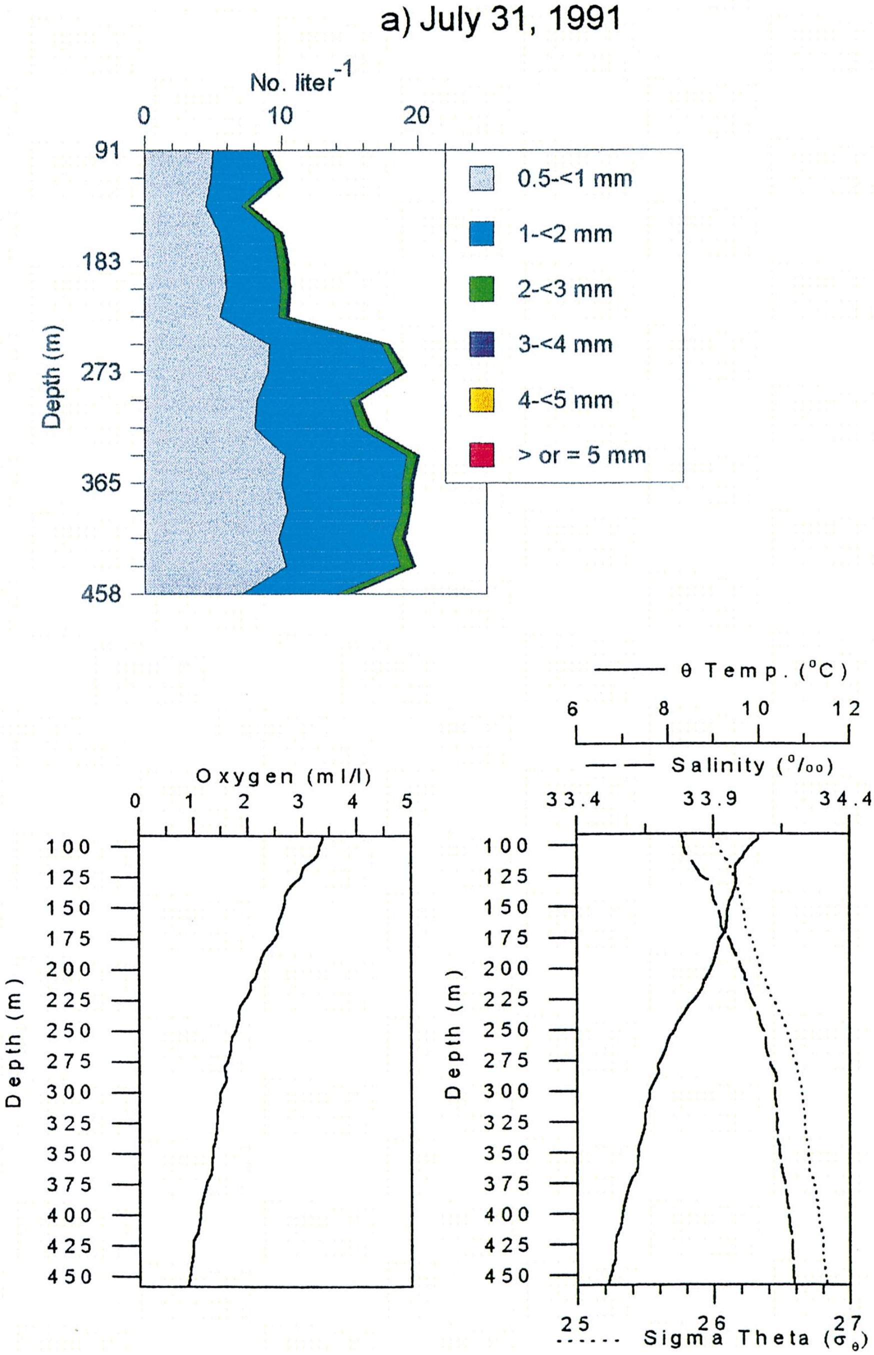
a) July 31, 1991
No. liter-1
0
10
20
Depth (m)
91
183
273
365
458
0.5-<1 mm
1-<2 mm
2-<3 mm
3-<4 mm
4-<5 mm
> or = 5 mm
Oxygen (ml/l)
θ Temp. (°C)
Salinity (°/oo)
Sigma Theta (σθ)
100
125
150
175
200
225
250
275
300
325
350
375
400
425
450
33.4
33.9
34.4
25
26
27

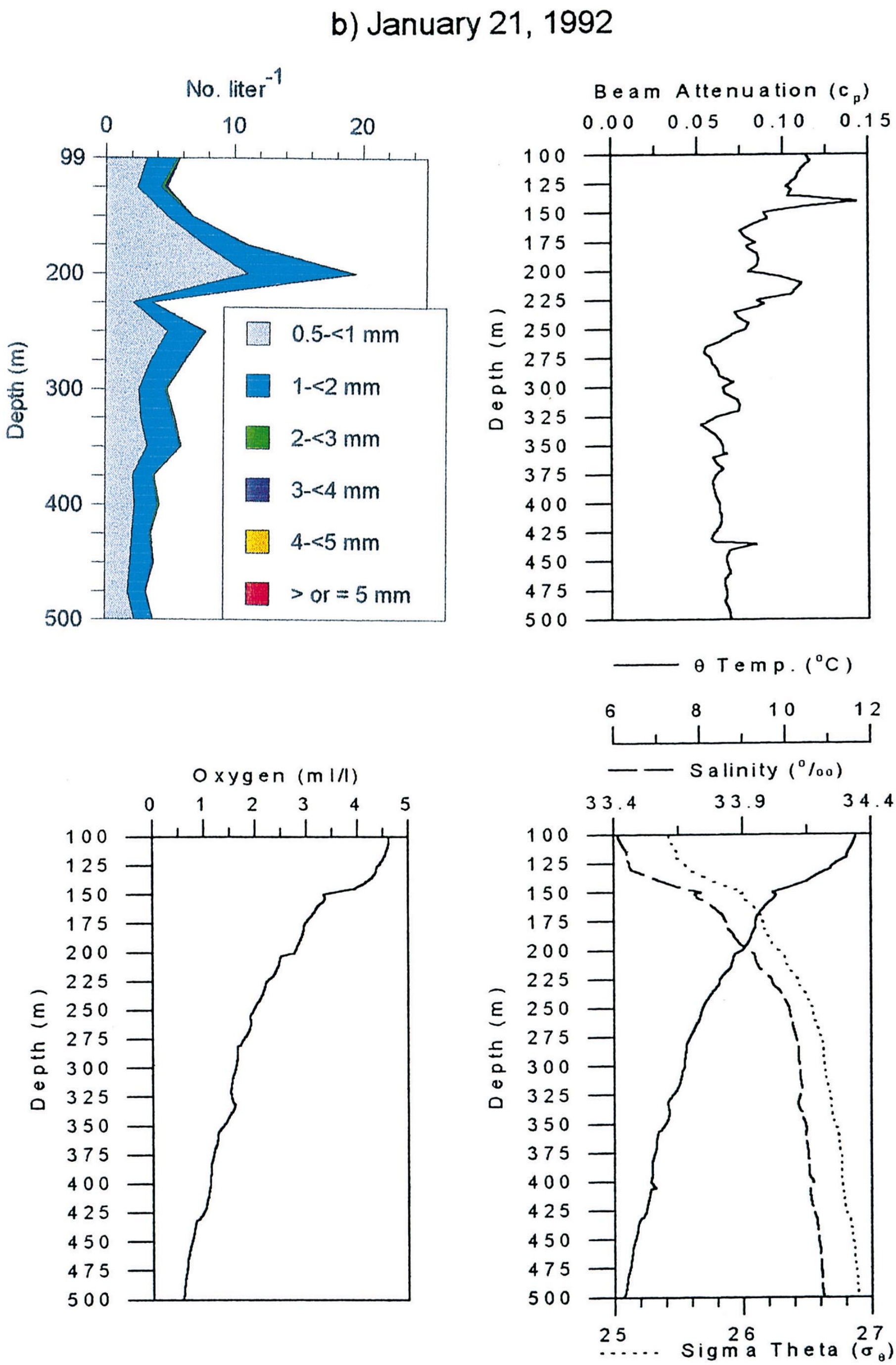

Fig. 6. Continued.

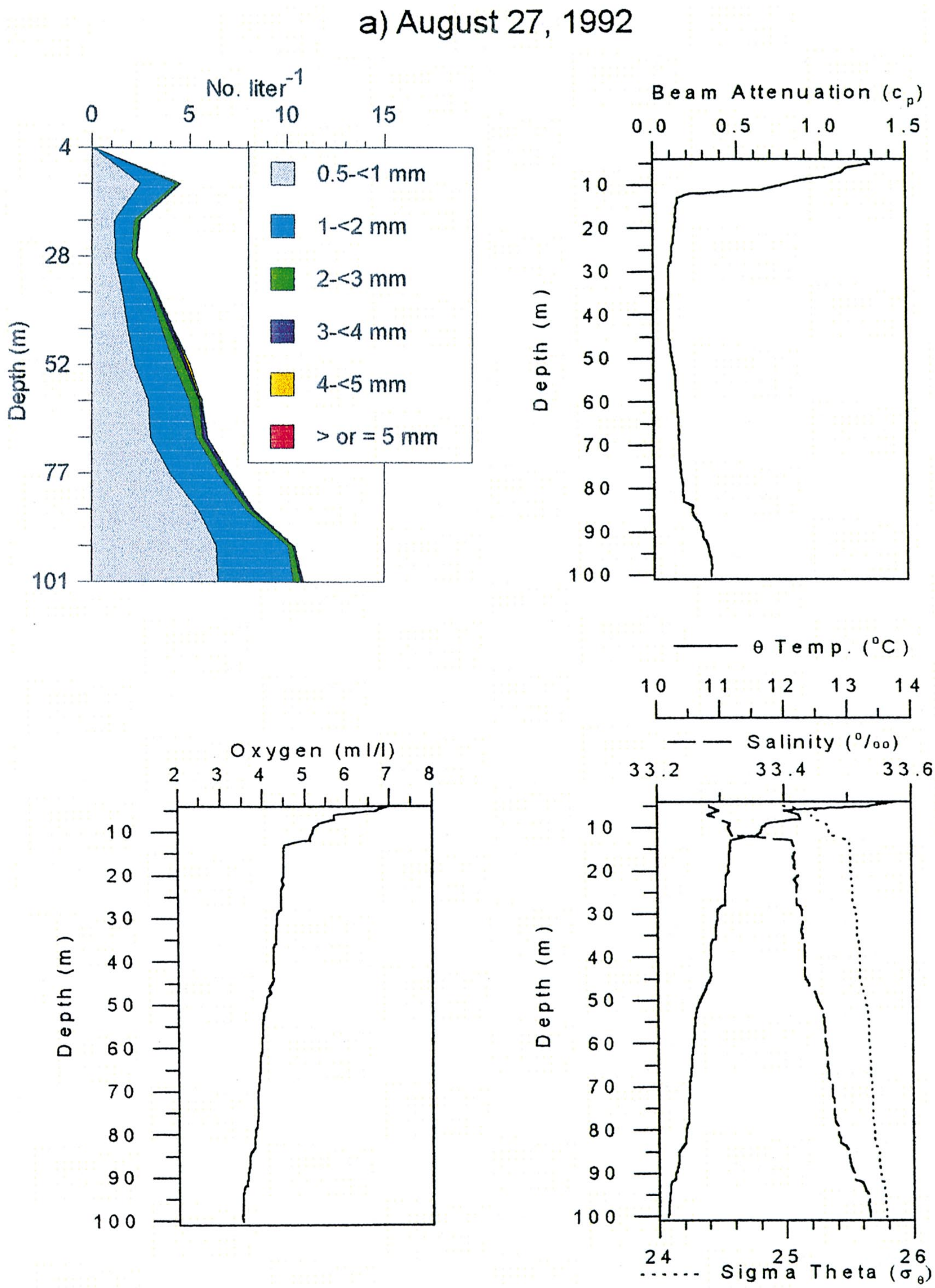

Fig. 7. Night-time upper water column (~ 1–100 m) aggregate abundance profiles and simultaneously collected hydrographic and c_p profiles obtained on (a) 8/27/92 and (b) 8/28/97 in Monterey Bay showing shallow aggregate peaks associated with pycnocline depth.

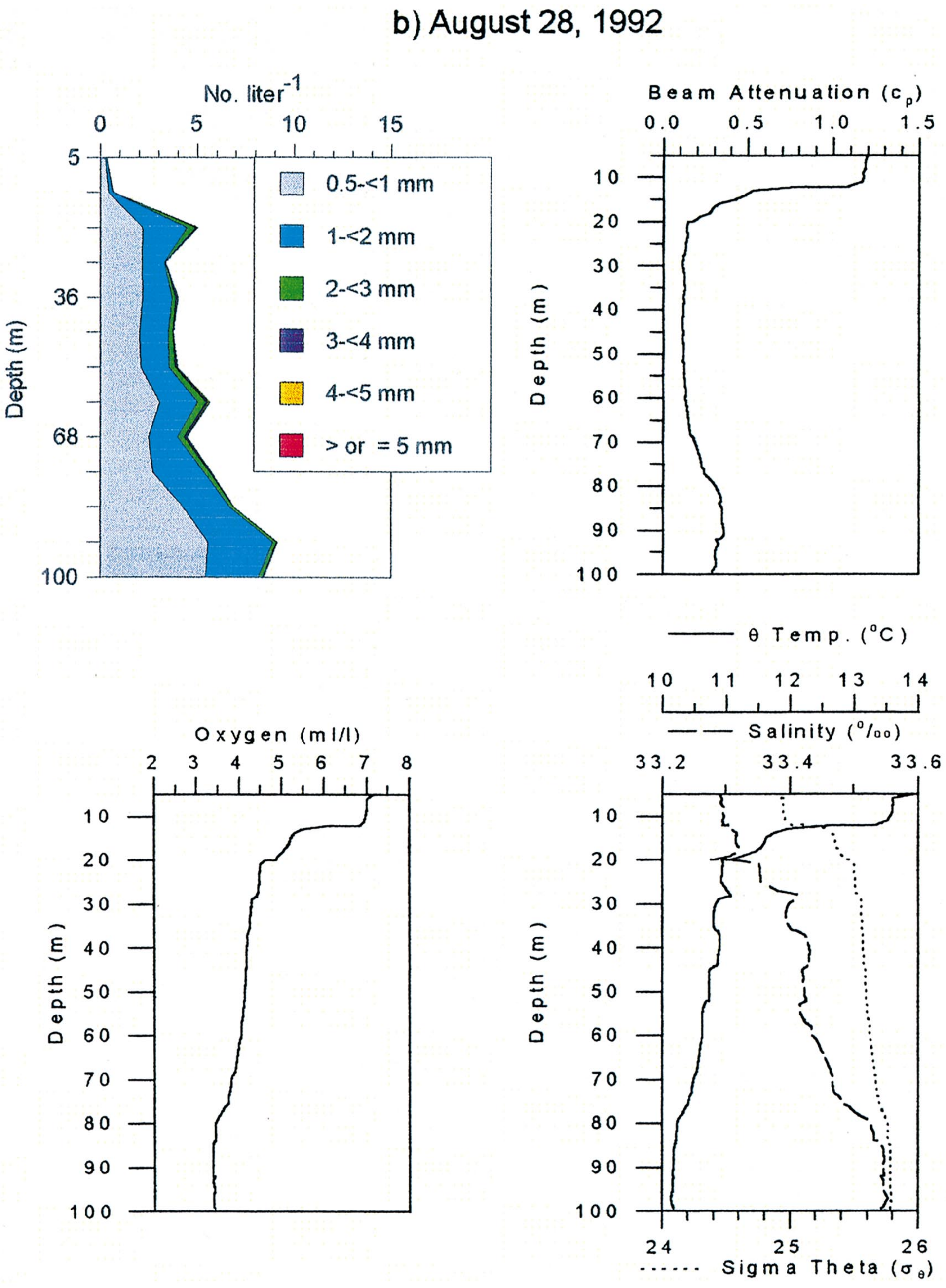

Fig. 7. Continued.

smaller amount of trap-collected sinking particulates consisted of zooplankton fecal pellets and amorphous organic debris completely lacking in diatoms but containing small picoplankton and nanoplankton components such as small *Nitzschia* spp. tests, small dinoflagellates, and *Synechococcus* spp. (Chavez, 1996; Pilskaln et al., 1996). If the trap had collected an appreciable amount of resuspended and laterally advected particle aggregates originating on the shelf/slope region, this would have been clearly evidenced in the microscopic, geochemical, and isotopic composition of the collected particulate material. Studies conducted in regions where the lateral input of particulate material at depth was determined to be a significant process, have documented the various geochemical signatures and distinguishing microscopic characteristics of relatively fresh planktonic POM versus resuspended and laterally advected particulate material. Laterally advected, resuspended particulates are distinguished by their low labile POC content, high C/N ratios, uncoupled $\delta^{15}N$ values of the trap material versus sub-euphotic zone NO_3^-, and etched microfossil appearance (Honjo, 1982; Honjo et al., 1982a–c; Walsh et al., 1988; Asper et al., 1992; Altabet, 1996; Pilskaln et al., 1998). In the case of the settling particulate material collected in the S1 Monterey Bay time-series trap over the same time period when the nearby aggregate study was conducted, the chemical and microscopic evidence all pointed to a predominantly seasonal, planktonic source of the water column POM (Pilskaln et al., 1996; Altabet et al., in prep.).

Finally, if resuspension and lateral advection from the shelf and slope areas of Monterey Bay were providing significant contributions to the sinking aggregate population examined in this study, one might expect to observe aggregate peaks during the non-upwelling/low productivity months of October through January. This represents the time period when rainfall levels are high, terrestrial sediment run-off into the Bay is maximized, and turbid plumes are observed extending up to 10 km offshore (Pilskaln et al., 1996). The S1 trap-measured particulate lithogenic fluxes in fact displayed peaks during the winter months of 1990 and 1991 and the lithogenic content of the trap material was quite high over all seasons (Pilskaln et al., 1996). The latter was attributed to the passive scavenging of suspended lithogenic matter from the coastal margin water column by seasonally produced, sinking POM (Pilskaln et al., 1996). However, the aggregate abundance profiles obtained during these months were essentially featureless, displaying minimal aggregate abundance values throughout the midwater column in comparison to the spring and summer month profiles (Figs. 4 and 5).

Based on all of the above evidence, it is our contention that the midwater aggregate peaks documented in the present study and primarily occurring during the productive spring and summer months, represent the temporal signal of sinking aggregate populations produced in the overlying upper water column. Supporting this is a significant positive correlation ($r = 0.7$) observed in 1991 between aggregate peak abundance and primary production, the latter measured and averaged over an approximate two week period encompassing the monthly aggregate profiling date. For the 1992 El Niño year data sets, the same correlation is positive but not significant ($r = 0.2$), suggesting a cause and effect disconnection between the quantitative coupling of primary production, aggregate formation and settling, and measured POC fluxes in 1992 as discussed in Pilskaln et al. (1996) and Silver et al. (1998). Silver et al. (1998) examines this apparent disconnection in Monterey Bay on a relatively short, instantaneous temporal scale through a study of aggregate composition in twelve samples collected in the midwater, 50% of which were obtained during the extended, low level El Niño period between 1992 and 1994. Additionally, a plankton dynamics model presented by Olivieri and Chavez (1998) indicates that the only phytoplankton material which effectively sinks out of the euphotic zone in this coastal upwelling system, must do so as detrital aggregate material as the individual sinking rates of algal cells and chains are not great enough to overcome average upwelling velocities of 5.6 m day^{-1}. The results of the computer model presented in this latter study confirm the findings presented in the POC budget model of Pilskaln et al. (1996) that in the Monterey Bay upwelling system, a much larger proportion of the primary production POC is transported offshore via strong, advective, near-surface flows, than that which is exported below the euphotic zone in the form of sinking marine aggregates and fecal pellets.

3.3. Aggregate sinking rates: Relationship to aggregate size and shape

Examples of the plots generated during the aggregate sinking rate experiments by the time-dependent loss of aggregates observed within the structured light volume inside the settling chamber, are shown in Fig. 8a and b (9 August 1993 experiments at 200 and 500 m). A total of 1023 aggregates were analyzed in the sinking rate experiments which included: 505 aggregates of 0.5 to $<$ 1.0 mm in size, 422 of 1.0 to $<$ 2.0 mm in size, 67 of 2.0 to $<$ 3.0 mm in size, 16 of 3.0 to $<$ 4.0 mm in size, 8 of 4.0 to $<$ 5.0 mm, and 5 within the $\geqslant$ 5.0 mm size class. We felt that the small sample size (5) of the largest aggregate size class ($>$ 5.0 mm), examined in the sinking rate experiments, was too small for us to obtain a robust set of sinking rates.

Cumulative mean aggregate sinking rates for the five aggregate size classes between 0.5 and $<$ 5.0 mm measured at the five sinking rate survey depths are presented in Table 1. The mean sinking rate values given in the table are weighted means based on either the relative numerical abundance of aggregates within each size class at a particular survey depth, or the relative numerical abundance over the five survey depths of aggregates all within the same size class. A comparison of the ranges of the means for the depth versus size class-averaged sinking rates indicates that midwater particle sinking rates display greater variation as a function of size class as opposed to water column depth. Such a finding is not surprising considering the lack of prominent density features within the midwater region of Monterey Bay, which potentially could exert an important influence over aggregate sinking rates and aggregate abundance distribution with depth (MacIntyre et al., 1995).

A regression of aggregate size class (over the range of 0.5 to $<$ 5.0 mm) versus sinking rate reveals a positive relationship between aggregate sinking rate and aggregate diameter (Fig. 9). This finding agrees with the aggregate sinking rate/size trend reported by Alldredge and Gotschalk (1988) for populations of surface water aggregates examined off Southern California A comparison of our aggregate sinking rates with those reported by Shanks and Trent (1980) and Alldredge and Gotschalk (1988) revealed substantially higher rates reported in the latter two studies, both of which were conducted in surface waters off California using SCUBA techniques. The vast majority of the 80 individual aggregate sinking speeds reported by Alldredge and Gotschalk (1988) for 2.0–5.0 mm-sized aggregates were greater than 40 m d^{-1}. For essentially the same aggregate size range, Shanks and Trent (1980) reported sinking rates that exceeded 50 m d^{-1} based on individual aggregate measurements completed in settling tubes at the depth of aggregate collection. These compare to our sinking rate values of 16–25 m day^{-1} determined for aggregates within the five size classes between 0.5 and < 5.0 mm aggregate diameter (Table 1). Similar to our results, Asper (1987) also showed slower sinking rates for midwater aggregates relative to those reported from surface water studies. Based on in-situ measured aggregate

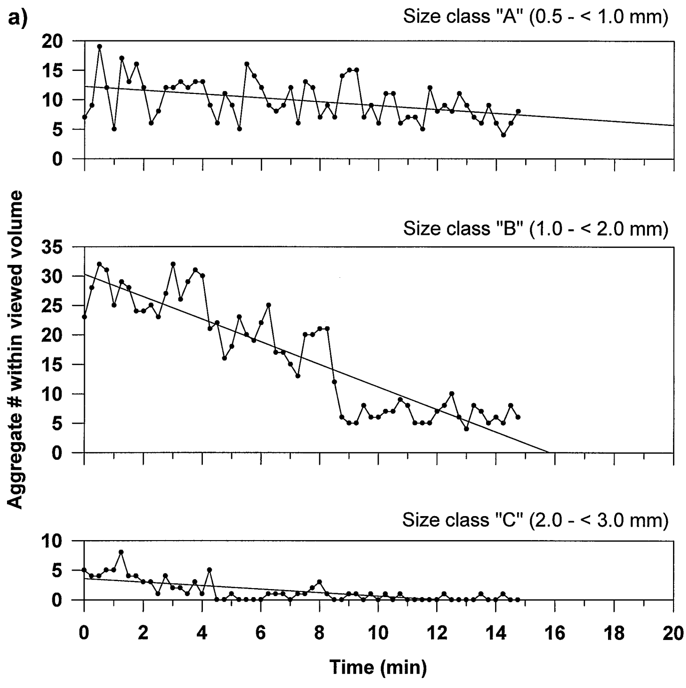

For plots above, where y = ax + b

Size class	Slope (a)	Y-intercept (b)	Time (min) when y = b/2 (x)	Velocity cm sec^{-1}	Velocity m day^{-1}
A	-0.330	12.230	18.530	0.012	10.025
B	-1.920	30.310	7.893	0.027	23.534
C	-0.290	3.560	6.138	0.035	30.264

Fig. 8. Sinking rate experiment results from 8/9/93 for (a) 200 m and (b) 500 m showing number of aggregates viewed within chamber over time for several aggregate size classes. Tables provide equation for the least-squares regression line in each plot and resultant size class sinking rates.

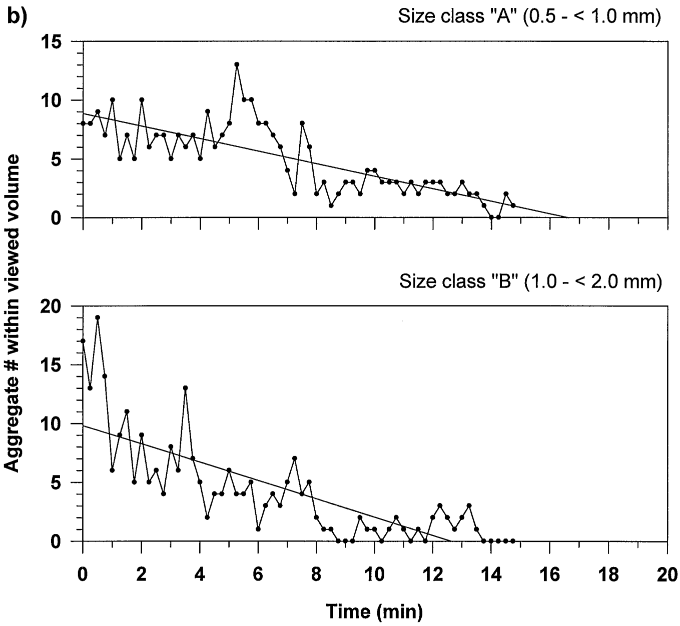

For plots above, where y = ax + b

Size class	Slope (a)	Y-intercept (b)	Time (min) when y = b/2 (x)	Velocity cm sec^{-1}	Velocity m day^{-1}
A	-0.530	8.850	8.349	0.026	22.249
B	-0.780	9.820	6.295	0.034	29.510

Fig. 8. Continued.

abundance flux at 380 , Asper (1987) calculated sinking rates of 26–36 m day^{-1} for aggregates of 1.0–4.0 mm in size, which are quite comparable to our midwater rates (Table 1).

The differences between the aggregate sinking rates provided by our study and that of Asper (1987), versus those provided in Alldredge and Gotschalk (1988) and Shanks and Trent (1980), may reflect an overall decrease in settling rate between surface water and mid-depth aggregate populations. Depending upon the specific environmental setting, a number of inter-related factors could contribute to such a trend: depth-variable rates of physical disaggregation and chemical remineralization of aggregates, the structure of the mid-water consumer community, lateral input at depth of partially remineralized, slowly settling aggregates, depth variable rates of fluid shear, and aggregate size and shape changes with depth (Asper, 1987; Alldredge and Silver, 1988; Alldredge et al., 1990; Lampitt et al., 1993).

Key methodological differences between our sinking rate experiments and those of Shanks and Trent (1980) and Alldredge and Gotschalk (1988) probably contributed significantly to the variations observed between the studies in the sinking rates

Table 1
Cumulative mean aggregate sinking rates (m d^{-1}) by size class and depth

Depth (m)	Size Class					Mean[a]	S.D.
	0.5–< 1.0 mm	1.0–< 2.0 mm	2.0–< 3.0 mm	3.0–< 4.0 mm	4.0–< 5.0 mm		
100	13.43	22.92	28.36	20.80	24.64	21.42	± 9.89
200	14.72	21.49	23.55	27.33	22.23	21.37	± 8.19
300	19.24	17.70	23.53	20.64	21.30	20.05	± 6.86
400	20.30	23.27	22.93	20.74	26.92	22.69	± 4.81
500	14.58	23.38	17.86	36.47	34.82	21.75	± 8.70
Mean[b]	16.29	21.92	24.53	23.99	25.46		
S.D.	± 5.70	± 7.97	± 9.64	± 6.40	± 8.00		

[a] Weighted means based on relative abundance of aggregates within different size classes at one depth.
[b] Weighted means based on relative abundance at different depths of aggregates within one size class.

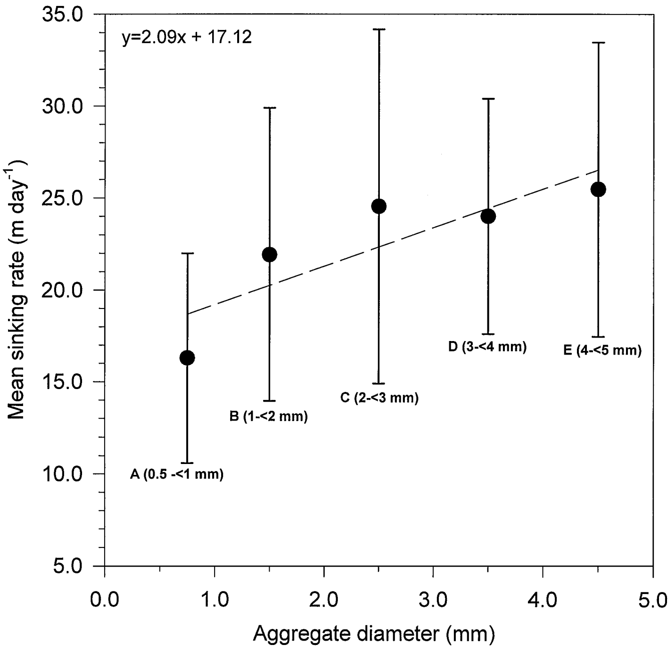

Fig. 9. Plot of aggregate size class (0.5–< 5.0 mm) versus mean sinking rate ($n = 1018$ aggregates). Solid circles are the size class means, vertical bars represent standard deviations.

reported for aggregates of similar size. Firstly, the total number of aggregates (> 1000) examined in our midwater chamber experiments is over an order of magnitude greater than what has been possible with surface water investigations of aggregate settling rates using SCUBA techniques. Secondly, our sinking rate experiments, based on loss rate over time of a particular size class population as a function of sinking, account for that subset of the population that may not have been sinking and/or may have been sinking at negligible speeds (Asper, 1987). These key aspects of our experiments enable us to determine true size class population sinking rates, something that has not been possible with SCUBA-based studies that examine individual aggregate sinking rate and are limited by sample size. Therefore our sinking rates are more representative of the naturally occurring size class population as compared to individual aggregate sinking rates.

The potential relationship between aggregate shape, size, sinking rate, and depth of sinking was examined using 716 aggregates involved in the sinking rate experiments for which a circularity value (P^2/A) was measured by the Optimas program. The 716 aggregates were sampled from video images selected from the beginning of each sinking rate experiment. Due to the fact that spheres sink more rapidly than aggregates of equivalent spherical diameter, it has been hypothesized that aggregate shape may be a factor affecting individual settling velocity as a function of shape-induced changes in drag coefficient (Komar and Reimers, 1978, Alldredge and Gotschalk, 1988). Studies by Komar and Reimers (1978) and Alldredge and Gotschalk (1988) have examined the hypothesis that particle drag coefficient should increase and sinking rate decrease as a function of decreasing spherical shape for marine particles. Additionally, trends in aggregate shape may be related to size class wherein smaller aggregates more closely approach a spherical shape and larger aggregates deviate from a spherical to a more elongate or comet-like shape (Alldredge and Silver, 1988). A possible corollary to these findings would be that as larger aggregates sink through the water column, their shape may become more elongated in the direction of sinking due to frictional drag forces. Thus we hypothesized that deeper-collected aggregates, presumably sinking over longer periods of time than shallow-collected aggregates, might exhibit a more elongate shape. Statistical tests were completed on the in situ aggregate data sets of size, sinking rate, depth of sinking, and circularity to determine if there were any observable trends in these properties. An ANOVA test of the sinking rate data set was not possible due to the fact that the population did not exhibit a normal distribution. A less rigorous, Friedman's non-parametric two-way analysis of variance of the sinking rate data set did reveal size class and depth effects on aggregate circularity at the 95% confidence level. But the Friedman's test does not specifically indicate where these differences may lie, i.e. between which particular size classes or particular depths, and as such, the results of the analysis were not conclusive.

A plot of aggregate circularity versus aggregate size for our midwater aggregate data set indicates a general trend of increasing deviation from circular (or spherical) shape with increasing aggregate diameter (Fig. 10). Komar and Reimers (1978) predicted a strong relationship between particle shape, drag, and sinking rate, but Alldredge and Gotschalk (1988) found no such relationship to exist in the case of surface water-collected marine snow particles. By comparison, our results suggest a relationship of decreasing particle circularity with increasing aggregate size and sinking rate over the size ranges which we examined (Figs. 9 and 10).

3.4. POC content of midwater aggregates

A total of 286 midwater-collected aggregates were collected using the ROV-mounted samplers and analyzed for organic carbon content (Table 2). The POC content of the individual aggregates was determined by dividing the total POC content of the filtered aggregate material obtained at one depth on a particular date by the number of aggregates collected. Our midwater aggregate POC values are highly variable between sample dates and depths, with a mean aggregate POC content of 1.56 ± 1.15 μg being slightly less than that reported in Alldredge and Silver (1988) of 2.65 μg POC aggregate^{-1} for surface water marine snow.

4. Discussion

4.1. Comparisons of Monterey Bay midwater aggregate abundance to previous studies

The aggregate profiles reported here for Monterey Bay display higher abundance values (e.g. number l^{-1}) than that previously reported by Honjo et al. (1984) for

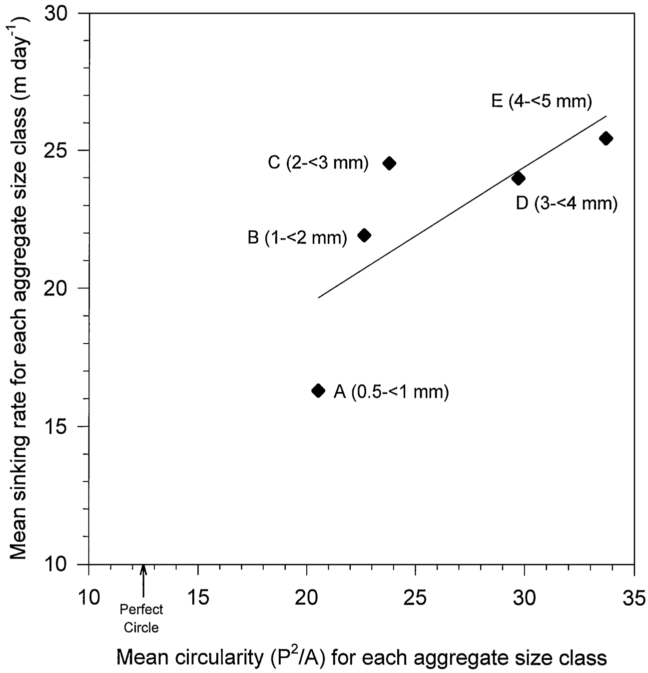

Fig. 10. Plot of mean aggregate circularity ($= P^2/A$) versus mean sinking rate for five aggregate size classes between 0.5–< 5.0 mm ($n = 716$ aggregates).

Table 2
Organic carbon content of mid-water marine aggregates: Monterey Bay

Sample date	Sample depth (m)	Total aggregates collected (#)	POC/aggregate (*u*g)
6/9/92	400	11	2.91
1/28/93	253	40	0.44
2/25/93	200	27	0.51
2/25/93	400	22	0.62
3/18/93	251	68	0.35
3/18/93	400	52	1.77
10/5/93	200	19	3.35
10/5/93	400	47	2.49
		Mean	1.56
		S.D.	1.15

comparable depths. In a normal upwelling year, we observed an abundance range of 5–20 aggregates l^{-1} in the summer months, as compared to < 5 aggregates l^{-1} for the 100–500 m depth range reported for July 1981 by Honjo et al. (1984). The Honjo et al. (1984) aggregate abundance profiles were more comparable to our 1992 El Niño year data sets where aggregate abundance values were often < 5 aggregates l^{-1}. A primary reason for the lower aggregate values reported by Honjo et al. (1984) relative to our values, may be attributed to substantial technique differences between the two studies. Honjo et al. (1984) employed a series of collimating Fresnel lenses to create a large collimated light volume within which aggregates were imaged. A drawback to collimated light and camera systems is that a perspection error exists whereby aggregates located at the front of the collimated light slab appear larger and aggregates near the back of the slab appear smaller (Honjo et al., 1984; Davis and Pilskaln, 1993). Therefore particle size must be estimated using the average distance to the middle of the illuminated volume rather than measuring actual particle size (Davis and Pilskaln, 1993). In an attempt to avoid this problem, the present study made use of a newly developed uncollimated light source consisting of a narrow, intense beam of light that was zoomable, focusable, and structured by a set of lenses and a rectangular mask (Davis and Pilskaln, 1993). Our study (versus Honjo et al., 1984) used a relatively small illuminated volume of light (2.2 l) with a limited volume thickness of 10 cm normal to the direction of the camera's view to ensure true size measurements of aggregates anywhere within a 95–105 cm distance from the camera. This distance was based on detailed calibrations of the focal distance and zoom angle of our high resolution, zoomable Sony video camera located 1 m from the center of the structured light beam (Davis and Pilskaln, 1993). By comparison, the Honjo et al. system imaged an extremely large (657 l) collimated light slab (40 cm thickness normal to the camera's view) that was photographed by a calibrated wide-angle still camera. Based on the substantial imaged volume differences, the perspection error associated with the collimated light system, and the camera quality differences, it is reasonable to assume that the system of Honjo et al. (1984) may have "missed" a large number of aggregates contained within the collimated light field, especially smaller-sized aggregates (Asper, personal communication). Spatial and temporal patchiness in aggregate abundance also could have additionally contributed to the observed differences in the summer profiles from the two studies that were separated by a period of 10 y.

Significant differences were seen when we compared our two night-time 0–100 m aggregate profiles obtained in August 1992 to the 0–100 m night profile presented in MacIntyre et al. (1995) for April 1990. Our pycnocline-associated aggregate peaks of 5 aggregates l^{-1} were much lower than that reported by MacIntyre et al. (1995), where values of > 40 aggregates l^{-1} were associated with a 20 m density discontinuity layer (Fig. 7a and b). Our August 1992 sub-pycnocline aggregate abundance values were approximately 50% lower than those provided in the MacIntyre et al. (1995) April 1990 profile. Due to the similar technical aspects of the aggregate imaging systems used by us and by MacIntyre et al. (1995), the higher marine aggregate abundance values observed in April 1990 profile were most likely a reflection of the strong intra-annual variability in primary production, aggregate formation, and POM flux that occurred in the California coastal upwelling systems between 1990 and 1992 (Chavez, 1996; Pilskaln et al., 1996). 1990 was a normal upwelling year off central California with relatively high levels of spring and summer primary production and a strong correlation observed between production and POC export. Productivity, plankton community structure and POM export conditions were quite different during the El Niño year of 1992, and this was reflected in our 1991 versus 1992 aggregate abundance profiles (Chavez, 1996; Pilskaln et al., 1996; Fig. 4).

Lampitt et al. (1993) has completed the only seasonal midwater aggregate study to date, besides the Monterey Bay study presented here, in which monthly variations in aggregate abundance, volume, and size distribution were examined using an in situ profiling camera system. Our 1991 aggregate abundance and volume data sets from Monterey Bay displayed a similar magnitude of variation on a seasonal basis as that observed at 270 m in the Northeast Atlantic by Lampitt et al. (1993). A several-fold to order of magnitude change was observed in the total midwater aggregate abundance between low productivity seasons and spring bloom periods in both studies (Lampitt et al., 1993; Figs. 4 and 5). However in contrast to the findings by Lampitt et al. (1993), we found that a substantial portion of the overall seasonal variation in midwater aggregate abundance in the coastal upwelling environment off central California was primarily dependent upon variations in the abundance of the small (e.g. 0.5 to < 1.0 mm) and not the large-sized aggregates. Both the NE Atlantic and Monterey Bay studies document midwater aggregate volume peaks due to increases in the abundance of large aggregates (e.g. > 3.0 mm) during the months when primary production rates and particulate export are reported to be maximized (Lampitt et al., 1993; Pilskaln et al., 1996; Fig. 5). Aggregate data sets of sufficient temporal resolution ranging from days to months such as those from the Monterey Bay and Lampitt et al. (1993) studies provide strong support for the proposed link between phytoplankton bloom dynamics, the production of sinking algal aggregates and pulsed deliveries of POM to underlying waters (Alldredge and Gotschalk, 1989, 1990; Asper et al., 1992; Lampitt et al., 1993).

4.2. POC fluxes provided by aggregates in Monterey Bay

Using our mean POC content of midwater aggregates (Table 2), the aggregate abundance within each size class obtained at 450–458 m for each of the 15 profiles collected seasonally in 1991 and 1992 (from original data sets used to produce Fig. 4), and the aggregate sinking speeds for each size class averaged for the 400 and 500 m depth interval (Table 1), we calculated the flux of aggregate POC to 450 m for each month represented by the abundance profiles (Table 3). 450 m was the average depth of the Monterey Bay S1 time-series sediment trap deployed between 1989 and 1992, thus allowing us to compare the biweekly trap measure POC fluxes presented in Pilskaln et al. (1996) to those determined from the aggregate data sets presented here. Aggregate POC fluxes ranged from a high of over 400 mg POC m^{-2} d^{-1} calculated for the spring/summer of 1991, to a low of 24 mg POC m^{-2} d^{-1} obtained for January 1991 (Table 3). Comparing our seasonal aggregate POC fluxes to the biweekly, trap-measured POC fluxes at S1, we see that the aggregate fluxes are 2–7-fold larger than the trap fluxes obtained in the upwelling season and fall months, with more comparative values between the trap and aggregate-based fluxes observed during the non-upwelling winter months of December to February (Table 3).

Table 3
Calculated marine aggregate POC fluxes vs. trap-measured fluxes: *Monterey Bay* 1991–1992

Season	Month/yr	Marine aggregate POC flux ($mg\ m^{-2}\ d^{-1}$)	S1 450 m trap POC flux ($mg\ m^{-2}\ d^{-1}$)
Non-upwelling/winter	January 1991	26.3	[a]
	December 1991	66.2	55.2
Upwelling/spring–summer	March 1991	255.7	[a]
	April 1991	441.5	[a]
	June 1991	201.9	105.8
	July 1991	481.2	181.8
	August 1991	165.7	38.9
Non-upwelling/winter	January 1992	67.3	55.1
	February 1992	30.5	52.2
Upwelling/spring–summer	May 1992	266.9	34.2
	June 1992	203.1	58.8
	August 1992	122.6	78.8
Late upwelling/fall	September 1992	167.4	41.2
	October 1992	164.7	62.7

[a]No sediment trap sample collected.

Several important points regarding POC flux dynamics in the Monterey Bay/coastal central California region result from the above comparison and are discussed below. The obvious point is that the seasonal formation and sinking flux of marine aggregates produced primarily within the upper water column and defined within the size ranges studied here, are primarily responsible for the seasonal mass delivery of particulate organic carbon to mesopelagic depths in this productive, coastal upwelling system. It has been assumed by some that larger and more visually impressive particle aggregates such as the discarded outer houses of the giant pelagic larvacean, *Bathochordaeus*, frequently observed within the mesopelagic zone of Monterey Bay, are of significant importance to the annual deep-water delivery of organic matter in the region (Hamner and Robison, 1992). Quantitative results from this study, as well as two recently completed investigations of the chemical mass fluxes and numerical fluxes of algal cells and microorganisms associated with sinking *Bathochordaeus* houses, indicate that such assumptions are not supported by rigorous data sets (Silver et al., in press; Pilskaln et al., in prep.).

The large discrepancy in the aggregate-based and trap-measured POC fluxes must be explained. Clearly a portion of this discrepancy may be attributed to the significant temporal resolution differences existing between the aggregate POC fluxes and those measured by the S1 Monterey Bay trap. The aggregate fluxes are calculated from single day aggregate abundance measurements conducted over a period of hours, whereas the S1 trap fluxes were obtained from integrated biweekly collections of sinking particulate organic matter. Short-term, aggregate-based POC flux measurements may easily be biased by aggregate patchiness in time and space. Thus, the more time-integrated trap fluxes may better represent the mean monthly POC fluxes occurring in the region.

However, one also needs to consider the possibility that the subsurface, moored Monterey Bay cone-style trap under-collected the sinking aggregate population and thus the trap-measured POC fluxes were underestimated. This possibility was seriously considered by Pilskaln et al. (1996) in their determination of water column POC regeneration rates and presentation of an annual POC budget box model for Monterey Bay based on the S1 time-series trap data. Comparisons of the S1 data sets to previously determined POC fluxes, water column regeneration rates, independently measured benthic fluxes and carbon burial rates, and calculated *e*-ratios for the region, indicated that the resultant POC budget box model was reasonable based on all available data (Pilskaln et al., 1996). Data recently available from a Monterey Bay sediment trap intercomparison experiment, and a probability analysis of the collection efficiency by traps of different collection surface areas, provide information helpful to our resolution of the differences between the aggregate versus the trap POC fluxes. Pilskaln (in prep.) has estimated that the 0.05 m^2 diameter cone trap used in the S1 Monterey Bay time-series study underestimated the sinking midwater POC flux at by a factor of 1.5–2.0 relative to that measured by a large diameter (1.5 m^2) cone trap (e.g. typical JGOFS trap; Honjo and Doherty, 1988) deployed at a comparable depth [*Note*: Such an adjustment to the POC fluxes given in Pilskaln et al. (1996) would have an insignificant effect on the POC budget box model presented in the same study as neither the *e*-ratios nor the 0–500 m POC regeneration rates change by more than 3% of their reported values]. In a related study, Silver et al. (in press) have determined that a 0.05 m^2 collection area cone trap will accurately estimate the flux of large, rare sinking aggregates within a factor of two over a 2 week deployment, a large diameter 1.5 m^2 trap will do the same over a deployment period of several days, but traps with very small surface areas such as the VERTEX traps (collection surface of 0.0039 m^2) require deployments exceeding a month to measure accurately the flux of large particle aggregates within a factor of two.

If we assume that the S1 trap under-collected the sinking population of large aggregates when such aggregates were most abundant in the water column, i.e. the March–August maximum upwelling/high productivity period, and we increase the trap POC fluxes for these months in Table 3 by a factor of 2, we obtain a somewhat better comparison with the aggregate POC fluxes. Doubling the trap-measured POC fluxes measured during the winter/non-upwelling months is not warranted considering the relatively low abundance of aggregate material in the midwater during this time period, and the reasonably close agreement that already exists between the calculated aggregate and measured trap POC fluxes determined for these months (Fig. 4, Table 3). Even after applying a doubling factor to the trap POC fluxes, a number of the aggregate POC fluxes, especially those obtained in the spring to fall months of 1992, remain quite high by comparison. This finding is puzzling in light of the lower aggregate abundances that we have documented in 1992 versus 1991. A possible explanation may be that the aggregate fluxes for the upwelling to fall period of the 1992 El Niño year were overestimated by the use of aggregate sinking rates obtained after 1992.

Our sinking rate experiments were conducted during the latter part of 1993 and 1994 when hydrographic and productivity characteristics of the region were slowly returning to more normal, post-El Niño conditions (Chavez, personal communication). If the mid-water aggregate populations produced during the spring to early fall period of the 1992 El Niño were quite different in terms of size and composition from those produced during pre- and post-1992 El Niño years (i.e. 1991 and 1993, 1994), their sinking rates would conceivably reflect this. Chavez et al. (1996) and Pilskaln et al. (1996) provided evidence of the dramatic change in the composition of the phytoplankton and the sinking particulate organic matter between 1990/early 1991 and late 1991/1992. 1990 and early 1991 in Monterey Bay were typified by high productivity, diatom-dominated phytoplankton communities and an abundance of macrozooplankton consumers (Chavez, 1996; Pilskaln et al., 1996). In contrast, solitary picoplankton dominated the phytoplankton by early 1992 and microplankton grazers were the most abundant secondary consumers found in the water column (Chavez, 1996). One would expect that the sinking particle size spectrum resulting from a picoplankton-based community would be significantly smaller, aggregate abundance would likely be lower, and aggregate POM might be remineralized to a greater extent, and be less dense and of higher porosity than that produced by a high productivity, diatom-based system (Michaels and Silver, 1988; Chavez, 1996; Pilskaln et al., 1996). All of these factors could contribute to lower aggregate sinking rates, with the present study documenting on overall decrease in the size, abundance and volume of mid-water aggregates from 1991 to 1992. It is therefore possible that in contrast to 1991, the 1992 El Niño year aggregate population may have consisted of a significantly large subset of negligibly sinking and/or suspended aggregates to which we associated higher sinking rates based on our in situ settling rate experiments completed during post-El Niño years.

5. Conclusions

Over the past 20 yr, a substantial number of marine aggregate studies have been conducted in the waters of the California Current System using in situ SCUBA or aggregate imaging systems developed in the 1980s (Silver et al., 1978; Trent et al., 1978; Alldredge, 1979; Shanks and Trent, 1980; Alldredge and Cox, 1982; Prezlin and Alldredge, 1983; Honjo et al., 1984; Alldredge et al., 1986; Alldredge and Gotschalk, 1988; 1989; 1990; MacIntyre et al., 1995). The vast majority of these studies were concentrated in the 0–20 m surface water region, with two investigations extending to 100 m and deeper to examine midwater aggregate abundance (e.g. Honjo et al., 1984; MacIntyre et al., 1995). The combined results from these investigations have given us much insight into the temporal and spatial dynamics of marine aggregate abundance in the coastal California surface waters and the estimated flux of aggregate POC out of the upper water column. Their results have also emphasized the broader need for deeper water column studies and independent, in situ measurements of multiple aggregate properties coincident with time-series trap fluxes in order to quantitatively address the aggregate abundance versus flux question within a particular environmental setting (Asper, 1992; Walsh and Gardner, 1992).

Our study was unique in that it specifically addressed these needs with a first-time combination of seasonal aggregate abundance data, in situ measured sinking rates, and simultaneously collected trap fluxes, all concentrated primarily within the chemically dynamic, 100–500 m POC regeneration zone of the coastal California upwelling system. Additionally, our investigation was the first to make use of a sophisticated ROV for the in situ quantification of several midwater aggregate properties. The use of an ROV platform, while sacrificing fine-scale vertical resolution in aggregate data, provided a number of advantages over the more traditional aggregate profiling system of Honjo et al. (1984). What is gained from an ROV-based system is real-time monitoring of the data collection thus enhancing quality control for all properties measured, fine scale horizontal spatial information on aggregate abundance, and the ability to collect water column aggregates. The ROV-based data sets combined with the coincident time-series trap data enabled us to comprehensively quantify and assess the significance of POC fluxes provided by marine snow in the upwelling system off California. The results of this study considered along with the model of Olivieri and Chavez (1998) and the POC budget study of Pilskaln et al. (1996) underscore the importance of sub-euphotic zone aggregate fluxes as a means of delivering significant amounts of POM to the deep margin sediments of coastal upwelling systems – systems where the majority of the primary produced POC is transported from the local upwelling system by strong near-surface currents, prior to sinking out of the mixed layer.

Acknowledgements

We are extremely grateful to the following individuals without whom this field- and technology-intensive work could not have been accomplished: D. Davis, T. Gritton, R. Olivieri, K. Murphy,. J. Connor, S. Lowder, M. Yuen and D. Bracher for technical assistance and data analysis; D. Steinberg and S. Coale for their unending enthusiasm, ideas, and help on cruises and in the lab; T. Osborn for his short course on microscale turbulence and advice on sinking chamber design; MBARI ROV pilots J. McFarlane, C. Grech and T.C. Dawe, Capts. W. Wardle and M. VandenBerg, and the R/V Pt. Lobos crew for many successful and thoroughly enjoyable cruises; G. Burkhart, M. Parker and L. Mitchell for engineering and machine shop assistance. We thank A. Alldredge and R. Maffione for helpful discussions regarding experimental design and data quality control, V. Asper and I. Walsh for the same plus constructive reviews of the manuscript, and a third anonymous reviewer for his/her comments. This study was supported by NSF award OCE-9015602 and DOE grant DE-FG0392ER61449 to C. Pilskaln, NSF grants OCE-9012340 and OCE-9301892 to M. Silver, and funding at the Monterey Bay Aquarium Research Institute from the David and Lucile Packard Foundation.

References

Alldredge, A.L., 1979. The chemical composition of macroscopic aggregates in two neritic seas. Limnology and Oceanography 24, 855–866.

Alldredge A.L., Cox, J.L., 1982. Primary productivity and chemical composition of marine snow in surface waters of the Southern California Bight. Journal of Marine Research 40, 517–527.
Alldredge, A.L., Cole, J.J., Caron, D.A., 1986. Production of heterotrophic bacteria inhabiting macroscopic organic aggregates (marine snow) from surface waters. Limnology and Oceanography 31, 68–78.
Alldredge, A.L., Gotschalk, C.C., 1988. In-situ settling behavior of marine snow. Limnology and Oceanography 33, 339–351.
Alldredge, A.L., Silver, M.W., 1988. Characteristics, dynamics and significance of marine snow. Limnology and Oceanography 20, 41–82.
Alldredge, A.L., Gotschalk, C.C., 1989. Direct observations of the mass flocculation of diatom blooms: Characteristics, settling velocities and formation of diatom aggregates. Deep-Sea Research 36, 159–171.
Alldredge, A.L., Gotschalk, C.C., 1990. The relative contribution of marine snow of different origins to biological processes in coastal waters. Deep-Sea Research 10, 41–58.
Altabet, M.A., 1996. Nitrogen and carbon isotopic tracers of the source and transformation of particles in the deep-sea. In: Ittekot, V., Schafer, P., Honjo, S., Depetris, P.J. (Eds.), Particle Fluxes in the Ocean, Wiley, London, pp. 155–184.
Asper, V.L., 1987. Measuring the flux and sinking speed of marine snow aggregates. Deep-Sea Research 34, 1–17.
Asper, V.L., Honjo, S., Orsi, T.H., 1992. Distribution and transport of marine snow aggregates in the Panama Basin. Deep-Sea Research 39, 939–952.
Bishop, J.K.B., 1986. The correction and suspended matter calibration of Sea Tech transmissometer data. Deep-Sea Research 33, 121–134.
Bolin, R.L., Abbott, D.P., 1963. Studies on the marine climate and phytoplankton of the central coastal area of California. California Cooperative Fisheries Investigations 9, 23–45.
Broenkow, W.W., McKain, S.J., 1972. Tidal oscillations at the head of Monterey Submarine Canyon and their relation to oceanographic sampling and circulation in Monterey Bay. Moss Landing Marine Laboratories Technical Publication 72–5, 42 pp.
Chavez, F.P., 1996. Forcing and biological impact of onset of the 1992 El Niño in central California. Geophysical Research Letters 23, 265–268.
Chavez, F.P., Herlien, R., Thurmond, G., 1994. Oasis-acquisition system for mooring/drifters. Sea Technology 35, 51–60.
Davis, D.L., Pilskaln, C.H., 1993. Measurements with underwater video: camera and field width calibration and structured lighting. Marine Technology Society Journal 26, 13–19.
Davoll, P.J., Silver, M.W., 1986. Marine snow aggregates: life history sequence and microbial community of abandoned larvacean houses from Monterey Bay, California. Marine Ecology Progress Series 33, 111–120.
Dymond, J., Collier, R., 1988. Biogenic particle fluxes in the Equatorial Pacific: evidence for both high and low productivity during the 1982–1983 El Niño. Global Biogeochemical Cycles 2, 129–137.
Deuser, W.G., Ross, E.H., 1980. Seasonal changes in the flux of organic carbon to the deep Sargasso Sea. Nature 283, 364–365.
Fofonoff, N.P., Millard, R.C., 1983. Algorithms for computation of fundamental properties of seawater. UNESCO Technical Papers in Marine Science vol. 44, 53 pp.
Fowler, S.W., Knauer, G.A., 1986. Role of large particles in the transport of elements and organic compounds through the oceanic water column. Progress in Oceanography 16, 147–194.
Gardner, W.D., Walsh, I.D., 1990. Distribution of macroaggregates and fine-grained particles across a continental margin and their potential role in fluxes. Deep-Sea Research 37, 401–411.
Hamner, W.M., Robison, B.H., 1992. In-situ observations of giant appendicularians in Monterey Bay. Deep-Sea Research 39, 1299–1313.
Honjo, S., 1980. Material fluxes and modes of sedimentation in the mesopelagic and bathypelagic zones. Journal of Marine Research 38, 53–97.
Honjo, S., 1982. Seasonality and interaction of biogenic and lithogenic particulate flux at the Panama Basin. Science 218, 883–884.
Honjo, S., Manganini, S.J., Cole, J.J., 1982a. Sedimentation of biogenic matter in the deep ocean. Deep-Sea Research 29, 609–625.

Honjo, S., Manganini, S.J., Poppe, L.J., 1982b. Sedimentation of lithogenic particles in the open ocean. Marine Geology 50, 199–220.
Honjo, S., Spencer, D.W., Farrington, J.W., 1982c. deep advective transport of lithogenic particles in the Panama Basin. Science 216, 516–518.
Honjo, S., Doherty, K.W., Agarwal, Y.C., Asper, V.L., 1984. Direct optical assessment of large amorphous aggregates (marine snow. in the deep ocean. Deep-Sea Research 31, 67–76.
Knauer, G.A., Martin, J.H., Bruland, K.W., 1979. Fluxes of particulate carbon, nitrogen, and phosphorus in the upper water column of the northeast Pacific. Deep-Sea Research 26, 97–108.
Komar, P.D., Reimers, C.E., 1978. Grain shape effects on settling rates. Journal of Geology 86, 193–209.
Lampitt, R.S., Hiller, W.R., Challenor, P.G., 1993. Seasonal and diel variation in the open ocean concentration of marine snow aggregates. Nature 362, 737–739.
MacIntyre, S., Alldredge, A.L., Gotschalk, C.C., 1995. Accumulation of marine snow at density discontinuities in the water column. Limnology and Oceanography 40, 449–468.
Martin, J.H., Knauer,G.A., Karl, D.M., Broenkow, W.W., 1987. VERTEX: carbon cycling in the northeast Pacific. Deep-Sea Research 34, 267–285.
McCave, I.N. 1975. Vertical flux of particles in the ocean. Deep-Sea Research 22, 491–502.
Paduan, J.D., Rosenfeld, L.K., 1996. Remotely sensed surface currents in Monterey Bay from shore-based HF radar (CODAR). Journal of Geophysical Research 101, 20669–20686.
Pak, H.D., Kiefer, D.A., Kitchen, J.C., 1988. Meridional variations in the concentration of chlorophyll and microparticles in the North Pacific Ocean. Deep-Sea Research 35, 1151–1171.
Pillsbury, R., Pilskaln, C.H., Pittock, G., Still, R.E., 1992. Deep-water flow characteristics of Monterey Bay: a two-year current meter data set. Oregon State University Data Report 143, 92–2, 66 pp.
Pilskaln, C.H., Silver, M.W., Davis, D.L., Murphy, K.M., Lowder, S.A., Gritton, B. R., Lewis, L.M., 1991. A quantitative study of marine aggregates using specialized ROV instrumentation. Institute of Electrical and Electronic Engineers Proceedings 91CH3063–5, 1175–1182.
Pilskaln, C.H., Paduan, J.B., 1992. Laboratory techniques for the handling and geochemical analysis of water column particulate and surface sediment samples. Monterey Bay Aquarium Research Institute Technical Report 92–9, 22 pp.
Pilskaln, C.H., Paduan, J.B., Chavez, F.P., Anderson, R.Y., Berelson, W.M., 1996. Carbon export and regeneration in the coastal upwelling system of Monterey Bay, central California. Journal of Marine Research 54, 1149–1178.
Pilskaln, C.H., Churchill, J.H., Mayer, L.M., 1998. Resuspension of sediment by bottom trawling in the Gulf of Maine and potential geochemical consequences. Journal of Conservation Biology 12(6), 1051–1061.
Prezlin, B.B., Alldredge, A.L., 1983. Primary production of marine snow during and after an upwelling event. Limnology and Oceanography 28, 1156–1167.
Robison, B.H. 1993. Midwater research methods with MBARI's ROV. Marine Technology Society Journal 26, 32–39.
Rosenfeld, L.K., Schwing, F.B., Garfield, N., Tracy, D.E., 1994a. Bifurcated flow from an upwelling center: a cold water source for Monterey Bay. Continental Shelf Research 14, 931–964.
Rosenfeld, L.K., Schramm, R.E., Paduan, J.B., Hatcher, Jr. G.E., Anderson, T., 1994b. Hydrographic data collected in Monterey Bay during 1 September 1988 to 16 December 1992. Monterey Bay Aquarium Research Institute Technical Report 94–15, 549 pp.
Sea Tech, Inc., 1995. Transmissometer manual: 25 cm beam transmissometer serial number 649. Sea Tech, Inc., 19 pp.
Shanks, A.L., Trent, J.D., 1980. Marine snow: sinking rates and potential role in vertical flux. Deep-Sea Research 27, 137–144.
Silver, M.W., Shanks, A.L., Trent, J.D., 1978. Marine snow: microplankton habitat and source of small-scale patchiness in pelagic populations. Science 201, 371–373.
Strickland J.D.H., Parsons, T.R., 1972. A practical handbook of seawater analysis. Fisheries Research Board of Canada Bulletin 167, Ottawa, Canada, 311 pp.
Syvitski, J.P.M., Asprey, K.W., LeBlanc, K.W.G., 1995. In-situ characteristics of particles settling within a deep-water estuary. Deep-Sea Research 42, 223–256.

Trent, J.D., Shanks, A.L., Silver, M.W., 1978. In-situ and laboratory measurements on macroscopic aggregates in Monterey Bay, California. Limnology and Oceanography 23, 626–635.

Walsh, I.D., Fischer, K., Murray, D., Dymond, J., 1988. Evidence for resuspension of rebound particles from near-bottom sediment traps. Deep-Sea Research 35, 59–70.

Walsh, I.D., Gardner, M.D., 1992. A comparison of aggregate profiles with sediment trap fluxes. Deep-Sea Research 39, 1817–1834.